

Scaling the Kalman Filter for Large-Scale Traffic Estimation

Ye Sun, *Student Member, IEEE*, and Daniel B. Work , *Member, IEEE*

Abstract—This work introduces a scalable filtering algorithm for multiagent traffic estimation. Large-scale networks are spatially partitioned into overlapping road sections. The traffic dynamics of each section is given by the *switching mode model* using a conservation principle, and the traffic state in each section is estimated by a local agent. In the proposed filter, a consensus term is applied to promote interagent agreement on overlapping sections. The new filter, termed as (spatially) *distributed local Kalman consensus filter* (DLKCF), is shown to maintain *globally asymptotically stable* mean error dynamics when all sections switch among observable modes. When a section is unobservable, we show that the mean estimate of each state variable in the section is ultimately bounded, which is achieved by exploring the interaction between the properties of the traffic model and the measurement feedback of the filter. Based on the above results, the boundedness of the mean estimation error of the DLKCF under switching sequences with observable and unobservable modes is established to address the overall performance of the filter. Numerical experiments show the ability of the DLKCF to promote consensus, increase estimation accuracy compared to a local filter, and reduce the computational load compared to a centralized approach.

Index Terms—Consensus filter, distributed Kalman filter (KF), transportation networks.

I. INTRODUCTION

DESPITE important advances in sensing and computation, real-time traffic estimation problems are still open to a number of critical issues including:

- 1) the entire state of the transportation network is too large (usually of order at least 10^5) for the estimators to scale in real time;
- 2) few results are available that provide a theoretical analysis of the performance of traffic estimation algorithms; and
- 3) the nonobservability of the traffic model is inevitable due to the existence of shocks and the sparsity of sensor measurements.

This work aims at designing a scalable distributed traffic estimation algorithm to address issues 1) and 2) with specific care of issue 3). The large-scale network is partitioned into overlapping

sections, and the traffic density on each section evolves according to a conservation law traffic model. The density is estimated by a cheap commodity computer (referred hereafter as an agent) associated with each section. However, without coordination among agents, estimates provided by different agents inevitably disagree on the shared boundaries due to model and measurement errors. This potentially leads to problems where applications computed based on traffic estimates (e.g., navigation and traffic control) produce disparate results depending on which agents provide the estimates. To promote agreement between neighboring agents on their shared states, each agent shares sensor data and estimates with its neighbors, and a consensus term is introduced. The filter trades global optimality in favor of scalability both in terms of communication and computation, thus the proposed filter is suboptimal. Regardless, the proposed filter has performance guarantees when traffic state is observable or unobservable, as well as when the system switches between observable and unobservable modes. Specifically, in unobservable scenarios, the physical properties of the traffic model (i.e., mass conservation and a flow-density relationship) are combined with the measurement feedback in the correction step of the filter to analyse the theoretical performance of the filter.

Research on collaborative information processing is driven by the broad applications of multiagent systems. A complete communication network with all-to-all links is required in the *decentralized Kalman filter* [1], or relaxed in the *channel filter* [2] for the fixed tree communication topology. Recently, the application of consensus strategies in distributed estimation is widely studied to promote agreement on estimates among agents [3]–[5], and/or to reconstruct sensor data not directly accessible through purely sharing measurements with neighbors [6]–[8], thus approximating the central estimator. To ensure the stability of the estimators, each local system is assumed to be observable (or detectable) in [3]–[5], or the full system observability is only achieved given all the sensor data in the network [6]–[8]. A common feature of [1]–[8] is that all agents estimate the same full state of dimension n , which may not scale in large-scale traffic networks since the complexity of the *Kalman filter* (KF) is $O(n^3)$. Moreover, the nonobservability of the traffic model cannot be resolved even if all measurements throughout the network are fused.

There are also notable works on scalable distributed estimation algorithms, where each agent estimates (or performs computation on) a small subset of the full state. Specifically in [9] and [10], the large-scale state vector is partitioned into overlapping local states of dimension $n_l \ll n$, and the

Manuscript received August 2, 2016; revised January 20, 2017; accepted January 26, 2017. Date of publication February 14, 2017; date of current version September 17, 2018. This work is supported by the National Science Foundation under Grant CMMI-1351717. Recommended by Associate Editor Sonia Martinez.

The authors are with the Department of Civil and Environmental Engineering and Coordinated Science Laboratory, University of Illinois at Urbana-Champaign, Urbana, IL 61801 USA (e-mail: yesun@illinois.edu; dbwork@illinois.edu).

Color versions of one or more of the figures in this paper are available online at <http://ieeexplore.ieee.org>.

Digital Object Identifier 10.1109/TCNS.2017.2668898

computation task is distributed across local agents. In [9], the cross correlation of neighboring agents is incorporated in the estimation error covariance at the expense of requiring a $O(n_l^4)$ complexity at each local agent. However, the stability of the proposed estimator is not analyzed. In [10], a consensus term is designed to help each local agent reconstruct the estimates of other local states, and is analyzed only when all local filters are detectable and have achieved a steady state. Other relevant treatments include moving-horizon estimation [11] and distributed Kriged Kalman filtering [12]. However, they either require extensive communication, or rely on the statistics of random fields that are not directly applicable for traffic dynamics. Moreover, the estimators [11], [12] are not analyzed when the model is unobservable.

A number of sequential estimation algorithms has been applied for traffic monitoring. Due to the nonlinearity and non-differentiability [13] of the nonlinear hyperbolic conservation law used to describe traffic, few results exist that rigorously prove the performance of the proposed estimators. In [14], the discretized conservation law is transformed to a switched linear system known as the *switching mode model* (SMM), and the observability of each mode is analyzed. The properties of the error dynamics of a Luenberger observer in various modes of the SMM is given in [15], which inspires this work and is extended in [16], [17]. A recent overview of sequential estimation for scalar traffic models is given in [13]. Another interesting line of work focuses on designing estimators and associated numerical schemes directly for conservation laws, see [18] and references therein.

The main contribution of this paper is the design and analysis of a (spatially) *distributed local Kalman consensus filter* (DLKCF) (see Section III-B), with provable performance and neighbor consistency. The DLKCF is proposed to estimate traffic densities on large freeways, with the system dynamics described by the SMM (see Section II). We analyze the performance of the DLKCF under various observability scenarios, yielding three main results.

- 1) The dynamics of the mean estimation error is *globally asymptotically stable* (GAS) when all sections switch among observable modes of the SMM (see Section IV-A);
- 2) When a section switches among unobservable modes, the mean estimate is ultimately bounded inside a physically meaningful interval (see Section IV-B).
- 3) The mean estimation error is upper bounded for sections that switch among observable and unobservable modes, provided a minimum residence time in the observable mode(s) is satisfied (see Section IV-C).

The above results focus on the mean estimate and are derived based on the stability (or bounded partitions) of the estimation error covariances (given in the lemmas proceeding the propositions). Numerical results (see Section V) show the effect of the consensus term on reducing disagreement between estimates given by neighboring agents (with $\sim 50\%$ reduction), and that the DLKCF outperforms a purely *local KF* (LKF) on estimation accuracy.

Compared to our preliminary work [19], the main extension is to prove the overall performance of the DLKCF under switches among observable and unobservable modes. The DLKCF is also

modified to be scalable both in the sense of computation (i.e., with cubic computational complexity in the local dimension) and communication (i.e., each agent only communicates with its one-hop neighbors, and the global communication topology is not needed).

II. SCALAR MACROSCOPIC TRAFFIC MODELING

A. Cell Transmission Model

The classical conservation law describing the evolution of traffic density $\rho(t, x)$ on a road at location x and time t is the *Lighthill–Whitham–Richards partial differential equation* (LWR PDE) [20], [21]

$$\partial_t \rho + \partial_x \mathfrak{F}(\rho) = 0. \quad (1)$$

The function $\mathfrak{F}(\rho) = \rho v(\rho)$ is called the flux function, where $v(\rho)$ is an empirical velocity function used to close the model. The triangular flux function [22] used in this paper is given by

$$\mathfrak{F}(\rho) = \begin{cases} \rho v_m, & \text{if } \rho \in [0, \varrho_c] \\ w(\varrho_m - \rho), & \text{if } \rho \in [\varrho_c, \varrho_m] \end{cases} \quad (2)$$

where $w = \frac{\varrho_c v_m}{\varrho_m - \varrho_c}$, v_m denotes the *freeflow speed* and ϱ_m denotes the *maximum density*. The variable ϱ_c is the *critical density* at which the maximum flux is realized. For the triangular fundamental diagram, the flux function has different slopes in *freeflow* ($0 < \rho \leq \varrho_c$) and *congestion* ($\varrho_c < \rho \leq \varrho_m$). In freeflow, the slope is v_m , and in congestion, it is w .

The *cell transmission model* (CTM) [22] is a discretization of (1) and (2) using a Godunov scheme. Consider a discretization grid defined by a space step $\Delta x > 0$ and a time step $\Delta t > 0$. Let l index the cell defined by $x \in [l\Delta x, (l+1)\Delta x)$, and denote as ρ_k^l the density at time $k\Delta t$ in cell l , where $k \in \mathbb{N}$ and $l \in \mathbb{N}^+$. The discretized model (1) becomes

$$\rho_{k+1}^l = \rho_k^l + \frac{\Delta t}{\Delta x} (\mathfrak{f}(\rho_k^{l-1}, \rho_k^l) - \mathfrak{f}(\rho_k^l, \rho_k^{l+1})) \quad (3)$$

where $\mathfrak{f}(\rho_k^{l-1}, \rho_k^l)$ is the flux between cell $l-1$ and l

$$\mathfrak{f}(\rho_k^{l-1}, \rho_k^l) = \min\{v_m \rho_k^{l-1}, w(\varrho_m - \rho_k^l), q_m\} \quad (4)$$

where q_m is the maximum flow given by $q_m = v_m \varrho_c$. Note that if the *Courant–Friedrichs–Lewy* condition is satisfied, the solution of the CTM converges in L^1 to the weak solution of the LWR PDE as $\Delta x \rightarrow 0$.

B. Switching Mode Model

Consider a freeway section with n cells with the state variable at time step $k \in \mathbb{N}$ defined as $\rho_k = (\rho_k^1, \dots, \rho_k^n)^T$. The SMM [14] is derived from (1) under the main assumption that there is at most one transition between freeflow and congestion in each section. From an estimation point of view, the SMM also assumes the road network is partitioned into sections with sensors located in the first and last cell, such that the densities ρ_k^1 and ρ_k^n are directly measured. Finally, the SMM assumes the boundary density measurements are sufficiently accurate to distinguish between four of the five modes described next, but they cannot determine the precise location or direction of a shock.

Given the assumption of at most one transition in a section, the SMM may switch between the following five modes.

- 1) *Freeflow–freeflow*: (FF), in which all cells in the section are in freeflow.
- 2) *Congestion–congestion*: (CC), in which all cells in the section are in congestion.
- 3) *Congestion–freeflow*: (CF), in which the cells in the upstream part of the section (i.e., the cells in the upstream side of the transition between freeflow and congestion based on the direction of travel) are congested, and the cells in the downstream part are in freeflow.
- 4) *Freeflow–congestion 1*: (FC1), in which the upstream part of the section is in freeflow, the downstream part is in congestion, and the shock has positive velocity or is stationary.
- 5) *Freeflow–congestion 2*: (FC2), in which the upstream part of the section is in freeflow, the downstream part is in congestion, and the shock has negative velocity.

Note the boundary sensors cannot distinguish between modes 4) and 5).

In each mode stated above, the traffic state ρ_k evolves with linear dynamics, forming a hybrid system

$$\rho_{k+1} = A_{\sigma(k)}^{s(k)} \rho_k + B_{\sigma(k)}^{\rho, s(k)} \mathbf{1} \varrho_m + B_{\sigma(k)}^{q, s(k)} \mathbf{1} q_m \quad (5)$$

where $\mathbf{1}$ is the vector of all ones, and $A_{\sigma(k)}^{s(k)}$, $B_{\sigma(k)}^{\rho, s(k)}$, $B_{\sigma(k)}^{q, s(k)} \in \mathbb{R}^{n \times n}$ are to be defined precisely later. The index $\sigma(k) \in \mathcal{S}$, where $\mathcal{S} = \{\text{FF}, \text{CC}, \text{CF}, \text{FC1}, \text{FC2}\}$ is the set of the five modes, and $s(k) \in \{1, \dots, n-1\}$ is the index introduced to precisely locate the transition between freeflow and congestion when it exists. We say $s(k) = l$ when the transition occurs between cell l and $l+1$.

For all $p \in \{1, 2, \dots, n-1\}$, define $\Theta_p \in \mathbb{R}^{p \times p}$ and $\Delta_p \in \mathbb{R}^{p \times p}$ by their (i, j) th entries as

$$\Theta_p(i, j) = \begin{cases} 1 - \frac{v_m \Delta t}{\Delta x}, & \text{if } i = j \\ \frac{v_m \Delta t}{\Delta x}, & \text{if } i = j + 1 \\ 0 & \text{otherwise} \end{cases}$$

$$\Delta_p(i, j) = \begin{cases} 1 - \frac{w \Delta t}{\Delta x}, & \text{if } i = j \\ \frac{w \Delta t}{\Delta x}, & \text{if } i = j - 1 \\ 0 & \text{otherwise.} \end{cases}$$

In the FF mode, the mode index $\sigma = \text{FF}$, and the transition does not exist. The explicit forms of A_{σ}^s , $B_{\sigma}^{\rho, s}$, and $B_{\sigma}^{q, s}$ are

$$A_{\text{FF}} = \begin{pmatrix} 1 & \mathbf{0}_{1, n-1} \\ \left(\frac{v_m \Delta t}{\Delta x} \right) & \Theta_{n-1} \\ \mathbf{0}_{n-2, 1} & \end{pmatrix}, B_{\text{FF}}^{\rho} = B_{\text{FF}}^q = \mathbf{0}_{n, n}$$

where $\mathbf{0}_{n, m} \in \mathbb{R}^{n \times m}$, which is zero everywhere. In the CC mode, the transition also does not exist, and

$$A_{\text{CC}} = \begin{pmatrix} \Delta_{n-1} & \begin{pmatrix} \mathbf{0}_{n-2, 1} \\ \frac{w \Delta t}{\Delta x} \\ 1 \end{pmatrix} \\ \mathbf{0}_{1, n-1} & \end{pmatrix}, B_{\text{CC}}^{\rho} = B_{\text{CC}}^q = \mathbf{0}_{n, n}.$$

The FF (resp. CC) mode is observable given density measurement of the downstream (resp. upstream) cell.

In the CF mode, the mode index $\sigma = \text{CF}$, and

$$A_{\text{CF}}^s = \begin{pmatrix} \Delta_s & \mathbf{0}_{s, n-s} \\ \mathbf{0}_{n-s, s} & \Theta_{n-s} \end{pmatrix}, B_{\text{CF}}^{\rho, s} = \mathbf{0}_{n, n} + \frac{w \Delta t}{\Delta x} E_{s, s}$$

$$B_{\text{CF}}^{q, s} = \mathbf{0}_{n, n} - \frac{\Delta t}{\Delta x} E_{s, s+1} + \frac{\Delta t}{\Delta x} E_{s+1, s+1}$$

where $E_{i, j}$ are matrices that are zero everywhere but the (i, j) th entry, which is one. Note that s may take any value in $\{1, \dots, n-1\}$, depending on the location of the center of the expansion fan connecting the congested and freeflow states. The CF mode is observable given density measurements of the upstream and downstream cells.

In the two FC modes, define $\hat{\Theta}_p$ and $\hat{\Delta}_p$ as follows:

$$\hat{\Theta}_p = \begin{cases} \begin{pmatrix} 1 & \mathbf{0}_{1, p} \\ \left(\frac{v_m \Delta t}{\Delta x} \right) & \Theta_p \\ \mathbf{0}_{p-1, 1} & \end{pmatrix} & \text{if } p \in \{1, \dots, n-1\} \\ 1 & \text{if } p = 0 \end{cases}$$

and

$$\hat{\Delta}_p = \begin{cases} \begin{pmatrix} \Delta_p & \begin{pmatrix} \mathbf{0}_{1, p-1} \\ \frac{w \Delta t}{\Delta x} \\ 1 \end{pmatrix} \\ \mathbf{0}_{1, p} & \end{pmatrix} & \text{if } p \in \{1, \dots, n-1\}, \\ 1 & \text{if } p = 0. \end{cases}$$

When $\sigma = \text{FC1}$ and $s \in \{1, \dots, n-2\}$, or $\sigma = \text{FC2}$ and $s \in \{2, \dots, n-1\}$, the matrices A_{σ}^s , $B_{\sigma}^{\rho, s}$, and $B_{\sigma}^{q, s}$ read

$$A_{\sigma}^s = \begin{pmatrix} \hat{\Theta}_{\bar{s}-1} & \mathbf{0}_{\bar{s}, 1} & \mathbf{0}_{\bar{s}, \bar{s}} \\ \begin{pmatrix} \mathbf{0}_{1, \bar{s}-1} & \frac{v_m \Delta t}{\Delta x} \end{pmatrix} & 1 & \begin{pmatrix} \frac{w \Delta t}{\Delta x} & \mathbf{0}_{1, \bar{s}-1} \end{pmatrix} \\ \mathbf{0}_{\bar{s}, \bar{s}} & \mathbf{0}_{\bar{s}, 1} & \hat{\Delta}_{\bar{s}-1} \end{pmatrix}$$

$$B_{\sigma}^{\rho, s} = \begin{pmatrix} \mathbf{0}_{\bar{s}+1, \bar{s}+1} & \begin{pmatrix} \mathbf{0}_{\bar{s}, 1} & \mathbf{0}_{\bar{s}, \bar{s}-1} \\ -\frac{w \Delta t}{\Delta x} & \mathbf{0}_{1, \bar{s}-1} \end{pmatrix} \\ \mathbf{0}_{\bar{s}, \bar{s}+1} & \mathbf{0}_{\bar{s}, \bar{s}} \end{pmatrix}, B_{\sigma}^{q, s} = \mathbf{0}$$

where for $\sigma = \text{FC1}$ we have $\tilde{s} = s$ and $\bar{s} = n - s - 1$, and for $\sigma = \text{FC2}$ we have $\tilde{s} = s - 1$ and $\bar{s} = n - s$. When $\sigma = \text{FC1}$ and $s = n - 1$, we have $A_{\sigma}^s = \text{diag}(\hat{\Theta}_{n-2}, 1)$ (i.e., with $\hat{\Theta}_{n-2}$ and 1 on the diagonal), and $A_{\sigma}^s = \text{diag}(1, \hat{\Delta}_{n-2})$ when $\sigma = \text{FC2}$ and $s = 1$. For both cases, $B_{\sigma}^{\rho, s} = B_{\sigma}^{q, s} = \mathbf{0}_{n, n}$. The two FC modes are not observable unless density measurements of all the cells are available, which does not occur in practical discretizations of road networks.

For consistency with the shock dynamics in (1), the allowed mode transitions are enumerated in the graph constrained-SMM [16]. The results in this paper hold for the graph constrained and more general switching sequences.

The observability results of the SMM for individual modes can be derived directly from computing the rank of the observability matrix for each mode given (5) and the observation equation $z_k = H_k \rho_k$, where z_k is the measurement, and H_k is the appropriate output matrix. From a physical viewpoint, the nonobservability of the SMM is due to the irreversibility of the LWR PDE given the available sensor measurements in the presence of shocks, and is not due to the discretization.

III. DISTRIBUTED LOCAL KALMAN CONSENSUS FILTER

A. Kalman Filter

In this section, we briefly review the KF and introduce notations needed later in the proposed filter. Consider the linear time-varying system

$$\begin{aligned} \rho_{k+1} &= A_k \rho_k + \omega_k, \rho_k \in \mathbb{R}^n \\ z_k &= H_k \rho_k + v_k, z_k \in \mathbb{R}^m \end{aligned}$$

where $\omega_k \sim \mathcal{N}(0, Q_k)$ and $v_k \sim \mathcal{N}(0, R_k)$ are the white Gaussian model and measurement noise. Given the sensor data up to time k denoted by $\mathcal{Z}_k = \{z_0, \dots, z_k\}$, the *prior estimate* and *posterior estimate* of the state can be expressed as $\rho_{k|k-1} = \mathbb{E}[\rho_k | \mathcal{Z}_{k-1}]$ and $\rho_{k|k} = \mathbb{E}[\rho_k | \mathcal{Z}_k]$, respectively. Let $\eta_{k|k-1} = \rho_{k|k-1} - \rho_k$ and $\eta_{k|k} = \rho_{k|k} - \rho_k$ denote the prior and posterior estimation errors. The estimation error covariance matrices associated with $\rho_{k|k-1}$ and $\rho_{k|k}$ are given by $\Gamma_{k|k-1} = \mathbb{E}[\eta_{k|k-1} \eta_{k|k-1}^T | \mathcal{Z}_{k-1}]$ and $\Gamma_{k|k} = \mathbb{E}[\eta_{k|k} \eta_{k|k}^T | \mathcal{Z}_k]$. The KF sequentially computes $\rho_{k|k}$ from $\rho_{k-1|k-1}$ as follows:

$$\begin{aligned} \text{Prediction: } & \begin{cases} \rho_{k|k-1} = A_{k-1} \rho_{k-1|k-1} \\ \Gamma_{k|k-1} = A_{k-1} \Gamma_{k-1|k-1} A_{k-1}^T + Q_{k-1} \end{cases} \\ \text{Correction: } & \begin{cases} \rho_{k|k} = \rho_{k|k-1} + K_k (z_k - H_k \rho_{k|k-1}) \\ \Gamma_{k|k} = \Gamma_{k|k-1} - K_k H_k \Gamma_{k|k-1} \\ K_k = \Gamma_{k|k-1} H_k^T (R_k + H_k \Gamma_{k|k-1} H_k^T)^{-1}. \end{cases} \end{aligned}$$

B. Distributed Local Kalman Consensus Filter

In the DLKCF, the discretized freeway network is spatially partitioned into N overlapping sections, with each section estimated by its own agent. Neighboring agents are allowed to exchange measurements and state estimates to reduce disagreement on shared cells. For the one-dimensional freeway, the set of neighbors of section i is given by

$$\mathcal{N}_i = \begin{cases} \{i+1\}, & \text{if } i = 1 \\ \{i-1, i+1\}, & \text{if } i \neq 1, \text{ and } i \neq N \\ \{i-1\}, & \text{if } i = N. \end{cases} \quad (6)$$

Hence, the Laplacian associated with the communication topology is a tridiagonal matrix. The reader is referred to Fig. 1(d) for an illustration of the partitioning of a roadway into overlapping sections. In Fig. 1(d), the freeway is partitioned into seven sections with 28 cells and four sensors in each section, and there

are ten cells in each overlapping region between neighboring sections. Except for the agents associated with the first and last sections, each agent obtains direct measurements from the two boundary sensors in the section. For the other two sensors, their measurements are collected by the neighbors and sent to the agent.

Given the SMM, the system dynamics of section i reads

$$\rho_{i,k+1} = A_{i,k} \rho_{i,k} + B_{i,k}^\rho \mathbf{1} q_m + B_{i,k}^q \mathbf{1} q_m + \omega_{i,k} \quad (7)$$

where $A_{i,k} \in \mathcal{A} = \{A_{\text{FF}}, A_{\text{CC}}, A_s^s | \sigma \in \{\text{CF}, \text{FC1}, \text{FC2}\}, s \in \{1, 2, \dots, n-1\}\}$, $\rho_{i,k} \in \mathbb{R}^{n_i}$ and $\omega_{i,k} \sim \mathcal{N}(0, Q_{i,k})$ is the white Gaussian model noise. Note that in (7) and for the remainder of this paper subscript k for A , B^ρ , and B^q combines the effect of $\sigma(k)$ and $s(k)$, and subscript $i \in \{1, 2, \dots, N\}$ is the section index. The sensors are spatially distributed in the road network and measure the traffic density at their locations. Hence, if the p th sensor directly connected to agent i is located at the l th cell in section i , the p th row of $H_{i,k}^p$ is given by $(0, \dots, 0, 1, 0, \dots, 0)$, where the l th element is 1. The observation equation modeled at agent i that corresponds to the sensor data obtained by the sensors directly connected to agent j is given by

$$z_{j,k}^i = H_{j,k}^i \rho_{i,k} + v_{j,k}^i, z_{j,k}^i \in \mathbb{R}^{m_j}, j \in \mathcal{J}_i = \mathcal{N}_i \cup \{i\} \quad (8)$$

where $v_{j,k}^i \sim \mathcal{N}(0, R_{j,k}^i)$. Note that the sensor data $z_{j,k}^i$ for $j \in \mathcal{N}_i$ is obtained through receiving measurements from agent j . Consequently, through communication each agent possesses columnized sensor data $z_{i,k} = \text{col}_{j \in \mathcal{J}_i} (z_{j,k}^i)$ with noise $v_{i,k} = \text{col}_{j \in \mathcal{J}_i} (v_{j,k}^i)$ and a corresponding columnized output matrix $H_{i,k} = \text{col}_{j \in \mathcal{J}_i} (H_{j,k}^i)$, as well as a block diagonal measurement error covariance $R_{i,k} = \text{diag}_{j \in \mathcal{J}_i} (R_{j,k}^i)$.

For $j \in \mathcal{N}_i$, denote the dimension of the overlap between section i and j as $n_{i,j}$, and define the projection $\hat{I}_{i,j}$ as

$$\hat{I}_{i,j} = \begin{cases} (I_{n_{i,j}} \quad \mathbf{0}_{n_{i,j}, n_i - n_{i,j}}), & \text{if } j = i - 1 \\ (\mathbf{0}_{n_{i,j}, n_i - n_{i,j}} \quad I_{n_{i,j}}), & \text{if } j = i + 1 \end{cases} \quad (9)$$

where $I_{n_{i,j}} \in \mathbb{R}^{n_{i,j} \times n_{i,j}}$ is the identity matrix. The quantity $\hat{I}_{i,j} \rho_{i,k}$ selects the state of section i that overlaps with section j . A consensus term is added to the correction step of the DLKCF to promote agreement on estimates among neighboring agents on their shared overlapping regions. The prediction and correction steps of the DLKCF for agent i reads

$$\begin{cases} \rho_{i,k|k-1} = A_{i,k-1} \rho_{i,k-1|k-1} \\ \Gamma_{i,k|k-1} = A_{i,k-1} \Gamma_{i,k-1|k-1} A_{i,k-1}^T + Q_{i,k-1} \end{cases} \quad (10)$$

$$\begin{cases} \rho_{i,k|k} = \rho_{i,k|k-1} + K_{i,k} (z_{i,k} - H_{i,k} \rho_{i,k|k-1}) \\ \quad + \sum_{j \in \mathcal{N}_i} C_{i,k}^j (\hat{I}_{j,i} \rho_{j,k|k-1} - \hat{I}_{i,j} \rho_{i,k|k-1}) \\ \Gamma_{i,k|k} = \Gamma_{i,k|k-1} - K_{i,k} H_{i,k} \Gamma_{i,k|k-1} \\ K_{i,k} = \Gamma_{i,k|k-1} H_{i,k}^T (R_{i,k} + H_{i,k} \Gamma_{i,k|k-1} H_{i,k}^T)^{-1} \end{cases} \quad (11)$$

where $C_{i,k}^j$ is the *consensus gain* of agent i associated with neighbor j at time step k , and for simplicity we drop the middle two terms in (7), which are deterministic. Our choice of the

consensus gain is given by

$$C_{i,k}^j = \begin{cases} \gamma_{i,k}^j \Gamma_{i,k|k-1} \hat{I}_{i,j}^T & \sigma(k) \in \{\text{FF}, \text{CC}, \text{CF}\} \\ \mathbf{0}_{n_i, n_{i,j}} & \sigma(k) \in \{\text{FC1}, \text{FC2}\} \end{cases} \quad (12)$$

where $\gamma_{i,k}^j = \gamma_{j,k}^i$ is a sufficiently small scaling factor, with $\gamma_{i,k}^j < \gamma_{i,k}^*$ for all $i, j \in \mathcal{N}_i$ and k . The explicit form of $\gamma_{i,k}^*$ will be given in Proposition 1 to ensure the unbiasedness of the DLKCF. Under unobservable modes, the consensus term is turned off. According to (12), the consensus term is designed based on the belief of the current estimation accuracy and the disparity among neighbors on the prior estimate, thus promoting agreement on the state estimates. Although an arbitrary convex combination of the estimates between neighboring agents may considerably reduce disagreement, it may largely increase the estimation error. Hence, the scaling factor needs to be carefully designed to ensure stability of the DLKCF.

Remark 1: Given the consensus gain (12), one may derive the optimal Kalman gain $K_{i,k}$ through minimizing $\text{tr}(\Gamma_{i,k|k})$ in a similar way as Theorem 1 in [4], thus yielding an optimal DLKCF that incorporates the cross correlations among different agents in the estimation error covariance. However, the optimal DLKCF has large communication requirements (i.e., the cross covariance $\Gamma_{i,k|k}^j$ between section i and j needs to be computed by agent i for all $j \in \{1, \dots, N\}$) that conflicts the goal of designing a scalable traffic estimation algorithm. Moreover, when cross correlation terms are included, a section that is always observable can have an unbounded error covariance if the neighboring section is unobservable, as detailed in [23, Appendix A]. Instead, the Kalman gain $K_{i,k}$ in the DLKCF is noninteracting, resulting in a suboptimal filter. Nevertheless, it is shown in Proposition 1 that the GAS property of the error dynamics is not affected by neglecting the cross correlation terms. The consistency of the DLKCF is validated through exploring the average normalized (state) estimation error squared (NEES) measure [24] in Section V.

Before proving the properties of the estimator, the following assumptions are made for the DLKCF.

- 1) The state dimension $n_i \geq 2$ for all i since at least two boundary cells exist in each freeway section.
- 2) The noise models satisfy $q_1 I < Q_{i,k} < q_2 I$ and $r_1 I < R_{i,k} < r_2 I$ for all i and k , where q_1, q_2, r_1 , and r_2 are positive constants.
- 3) The scaling factor satisfies $\gamma_{i,k}^j \leq \hat{\gamma}_{i,k}^j = \hat{c} |\mathcal{N}_i|^{-1} \|\Gamma_{i,k|k-1} \hat{I}_{i,j}^T \mathbf{u}_{i,k}^j\|^{-1}$ in addition to $\gamma_{i,k}^j < \gamma_{i,k}^*$ for all $i, j \in \mathcal{N}_i$ and k .

Here $|\mathcal{N}_i|$ is the number of neighbors of agent i , and $\hat{c} > 0$ is a constant predefined to set an upper bound for the magnitude of the consensus term. Also note that the upper bound $\hat{\gamma}_{i,k}^j$ can be computed locally and online by each agent. In this case, the 2-norm¹ of the consensus term is upper bounded as follows:

$$\left\| \sum_{j \in \mathcal{N}_i} \gamma_{i,k}^j \Gamma_{i,k|k-1} \hat{I}_{i,j}^T \mathbf{u}_{i,k}^j \right\| \leq \hat{c}, \quad \text{for all } i \text{ and } k. \quad (13)$$

¹For the remainder of this paper, we denote as $\|\cdot\|$ the 2-norm of a matrix or a vector.

In practice, to run the DLKCF each agent needs to use $\hat{A}_{i,k}$ (i.e., the estimated $A_{i,k}$ obtained based on the state estimate and sensor data) instead of $A_{i,k}$ in (10). In observable modes, the matrix $A_{i,k}$ can be correctly reconstructed by the local agent. However, in the FC modes $\hat{A}_{i,k}$ and $A_{i,k}$ are unlikely to be the same since the agent also needs to estimate the location and direction of the shock. As a related note, using the constrained-CTM [16] can improve the estimation accuracy of $A_{i,k}$. Also note that all the theoretical performance analysis of the DLKCF regarding the unobservable scenarios in Section IV hold even if $\hat{A}_{i,k}$ and $A_{i,k}$ differ.

IV. STABILITY AND PERFORMANCE ANALYSIS OF THE DLKCF FOR TRAFFIC ESTIMATION

A. Asymptotic Stability of Mean Error in Observable Modes

Define the prior and posterior estimation error for section i as $\eta_{i,k|k-1} = \rho_{i,k|k-1} - \rho_{i,k}$ and $\eta_{i,k|k} = \rho_{i,k|k} - \rho_{i,k}$, and define the neighbor disagreement on the shared estimates as

$$\mathbf{w}_{i,k}^j = \hat{I}_{j,i} \eta_{j,k|k-1} - \hat{I}_{i,j} \eta_{i,k|k-1}. \quad (14)$$

Note that this is a different notion of disagreement from Corollary 1 of [4], which measures the disagreement of an agent's estimate with respect to the mean estimate over all the agents. The global estimation error $\boldsymbol{\eta}_{1:N,k|k}$ is constructed by $\boldsymbol{\eta}_{1:N,k|k} = \text{col}(\eta_{1,k|k}, \dots, \eta_{N,k|k})$. Let the bold font \mathbf{x} denote the mean of random vector x (i.e., $\mathbf{x} = \mathbb{E}[x]$). The mean of the estimation error in section i evolves as follows:

$$\boldsymbol{\eta}_{i,k|k} = F_{i,k} A_{i,k-1} \boldsymbol{\eta}_{i,k-1|k-1} + \sum_{j \in \mathcal{N}_i} C_{i,k}^j \mathbf{w}_{i,k}^j \quad (15)$$

where $F_{i,k} = I - K_{i,k} H_{i,k}$. We choose a *common Lyapunov function* candidate which reads

$$V_k = \sum_{i=1}^N \boldsymbol{\eta}_{i,k|k}^T \Gamma_{i,k|k}^{-1} \boldsymbol{\eta}_{i,k|k} \quad (16)$$

and compute its one-step change $\Delta V_k = V_k - V_{k-1}$ by applying (15) as follows:

$$\begin{aligned} \Delta V_k &= \sum_{i=1}^N \boldsymbol{\eta}_{i,k-1|k-1}^T \\ &\times \left(A_{i,k-1}^T F_{i,k}^T \Gamma_{i,k|k}^{-1} F_{i,k} A_{i,k-1} - \Gamma_{i,k-1|k-1}^{-1} \right) \boldsymbol{\eta}_{i,k-1|k-1} \\ &+ 2 \sum_{i=1}^N \left(\boldsymbol{\eta}_{i,k|k-1}^T F_{i,k}^T \Gamma_{i,k|k}^{-1} \sum_{j \in \mathcal{N}_i} C_{i,k}^j \mathbf{w}_{i,k}^j \right) \\ &+ \sum_{i=1}^N \left(\sum_{j \in \mathcal{N}_i} C_{i,k}^j \mathbf{w}_{i,k}^j \right)^T \Gamma_{i,k|k}^{-1} \left(\sum_{j \in \mathcal{N}_i} C_{i,k}^j \mathbf{w}_{i,k}^j \right). \end{aligned} \quad (17)$$

The next lemma is necessary to ensure that the common Lyapunov function (16) is *radially unbounded*.

Lemma 1: Consider a freeway section (indexed by i) that switches among observable modes for all $k \geq 0$. If $\Gamma_{i,0|0} > \mathbf{0}$,

then $\Gamma_{i,k|k}^{-1}$ given in the DLKCF (10) and (11) satisfies

$$\mathbf{0} < \mathbf{c}_1(\Gamma_{i,0|0}) I \leq \Gamma_{i,k|k}^{-1} \leq \mathbf{c}_2(\Gamma_{i,0|0}) I, \quad \text{for } k \geq 0 \quad (18)$$

independent of the switching sequence. The bounds $\mathbf{c}_1(\cdot)$ and $\mathbf{c}_2(\cdot)$ are functions of the initial estimation error covariance.

Proof: The bounds are constructed via Lemma 4.1 to Lemma 4.4 in the arXiv version of this paper [23]. ■

Proposition 1: Consider the DLKCF in (10) and (11) with the consensus gain in (12). Suppose all sections switch among the observable modes of the SMM. Then, the mean estimation error $\boldsymbol{\eta}_{1:N,k|k} = \mathbb{E}[\boldsymbol{\eta}_{1:N,k|k}]$ is GAS for sufficiently small $\gamma_{i,k}^j$.

Proof: When all sections switch among the observable modes, V_k is radially unbounded since (18) holds for all i . We show ΔV_k in (17) is negative definite when $\boldsymbol{\eta}_{1:N,k-1|k-1} \neq \mathbf{0}$.

Step 1: Negative definiteness of the first term in (17).

The proof for the first term follows closely from [4] with minor changes. Here, we only show the result and introduce the matrices needed in this paper. Note that $A_{i,k}$ is invertible for all i and k in the SMM. Each element in the first term in (17) can be equivalently written as (see Lemma 2 in [4] for a detailed derivation)

$$\begin{aligned} & \boldsymbol{\eta}_{i,k-1|k-1}^T \left(A_{i,k-1}^T F_{i,k-1}^T \Gamma_{i,k|k}^{-1} F_{i,k-1} A_{i,k-1} \right. \\ & \quad \left. - \Gamma_{i,k-1|k-1}^{-1} \right) \boldsymbol{\eta}_{i,k-1|k-1} \\ & = -\boldsymbol{\eta}_{i,k|k-1}^T \Lambda_{i,k-1} \boldsymbol{\eta}_{i,k|k-1} \end{aligned}$$

with $\Lambda_{i,k}$ defined as

$$\Lambda_{i,k} = (A_{i,k} \Gamma_{i,k|k} A_{i,k}^T)^{-1} - (A_{i,k} \Gamma_{i,k|k} A_{i,k}^T + W_{i,k})^{-1}$$

where $W_{i,k} = Q_{i,k} + \Gamma_{i,k+1|k} S_{i,k+1} \Gamma_{i,k+1|k} > 0$ and $S_{i,k} = H_{i,k}^T R_{i,k}^{-1} H_{i,k}$. Due to the matrix inversion lemma

$$\begin{aligned} & \Gamma_{i,k|k} A_{i,k}^T \Lambda_{i,k} A_{i,k} \Gamma_{i,k|k} \\ & = \Gamma_{i,k|k} - \Gamma_{i,k|k} A_{i,k}^T (A_{i,k} \Gamma_{i,k|k} A_{i,k}^T + W_{i,k})^{-1} A_{i,k} \Gamma_{i,k|k} \\ & = (\Gamma_{i,k|k}^{-1} + A_{i,k}^T W_{i,k}^{-1} A_{i,k})^{-1} > 0 \end{aligned}$$

hence $\Lambda_{i,k} > 0$. Consequently, the first term in (17) is negative definite.

Step 2: Negative semidefiniteness of the second term in (17).

Due to [4, Lemma 2(i)] we have $F_{i,k} = \Gamma_{i,k|k} \Gamma_{i,k-1}^{-1}$, hence the consensus gain is equivalent to

$$C_{i,k}^j = \gamma_{i,k}^j \Gamma_{i,k|k-1} \hat{I}_{i,j}^T = \gamma_{i,k}^j \Gamma_{i,k|k} (F_{i,k}^T)^{-1} \hat{I}_{i,j}^T.$$

Let $\hat{i} \in \{1, \dots, N-1\}$ be the index of the overlapping regions, and define $\hat{\boldsymbol{\eta}}_{i,k|k-1} = (\boldsymbol{\eta}_{i,k|k-1}^T \hat{I}_{i,\hat{i}+1}^T, \boldsymbol{\eta}_{i+1,k|k-1}^T \hat{I}_{i+1,\hat{i}}^T)^T$. The

second term in (17) can be written as

$$\begin{aligned} & 2 \sum_{i=1}^N \left(\boldsymbol{\eta}_{i,k|k-1}^T F_{i,k}^T \Gamma_{i,k|k}^{-1} \sum_{j \in \mathcal{N}_i} C_{i,k}^j \mathbf{u}_{i,k}^j \right) \\ & = 2 \sum_{i=1}^{N-1} \gamma_{i,k}^{\hat{i}+1} \left(\boldsymbol{\eta}_{i,k|k-1}^T \hat{I}_{i,\hat{i}+1}^T \mathbf{u}_{i,k}^{\hat{i}+1} + \boldsymbol{\eta}_{i+1,k|k-1}^T \hat{I}_{i+1,\hat{i}}^T \mathbf{u}_{i+1,k}^{\hat{i}} \right) \\ & = -2 \sum_{i=1}^{N-1} \gamma_{i,k}^{\hat{i}+1} \hat{\boldsymbol{\eta}}_{i,k|k-1}^T \hat{L}_i \hat{\boldsymbol{\eta}}_{i,k|k-1} \leq 0 \end{aligned}$$

where

$$\hat{L}_i = \begin{pmatrix} 1 & -1 \\ -1 & 1 \end{pmatrix} \otimes I_{n_{i,\hat{i}+1}}$$

and the last inequality holds due to the quadratic property of the Laplacian matrix [25].

Step 3: Upper bound of the third term in (17).

Given the choice of consensus gain in (12), we have

$$\begin{aligned} & \sum_{i=1}^N \left(\sum_{j \in \mathcal{N}_i} C_{i,k}^j \mathbf{u}_{i,k}^j \right)^T \Gamma_{i,k|k}^{-1} \left(\sum_{j \in \mathcal{N}_i} C_{i,k}^j \mathbf{u}_{i,k}^j \right) \\ & = \sum_{i=1}^N \left(\sum_{j \in \mathcal{N}_i} \hat{I}_{i,j}^T \gamma_{i,k}^j \mathbf{u}_{i,k}^j \right)^T G_{i,k} \left(\sum_{j \in \mathcal{N}_i} \hat{I}_{i,j}^T \gamma_{i,k}^j \mathbf{u}_{i,k}^j \right) \end{aligned}$$

where we define $G_{i,k} = A_{i,k-1} \Gamma_{i,k-1|k-1} A_{i,k-1}^T + Q_{i,k-1} + \Gamma_{i,k|k-1} S_{i,k} \Gamma_{i,k|k-1}$. Recall that $\mathcal{J}_i = \mathcal{N}_i \cup \{i\}$, and define $\boldsymbol{\eta}_{\mathcal{J}_i,k|k-1} = \text{col}_{j \in \mathcal{J}_i} (\boldsymbol{\eta}_{j,k|k-1})$, where j are sorted in ascending order. Columnizing $\mathbf{u}_{i,k}^j$ over all neighbors $j \in \mathcal{N}_i$ within section i yields

$$\mathbf{u}_{\mathcal{N}_i,k} = \text{col}_{j \in \mathcal{N}_i} (\gamma_{i,k}^j \mathbf{u}_{i,k}^j) = \tilde{L}_i \tilde{I}_i \boldsymbol{\eta}_{\mathcal{J}_i,k|k-1} \quad (19)$$

where j are sorted in ascending order, \tilde{L}_i is defined as

$$\tilde{L}_i = \begin{cases} \begin{pmatrix} -\hat{I}_{i,\hat{i}+1} & \hat{I}_{i+1,\hat{i}} \end{pmatrix}, & \text{if } i = 1 \\ \begin{pmatrix} \hat{I}_{i-1,\hat{i}} & -\hat{I}_{i,\hat{i}-1} \end{pmatrix}, & \text{if } i = n \\ \begin{pmatrix} \hat{I}_{i-1,\hat{i}} & -\hat{I}_{i,\hat{i}-1} & \mathbf{0}_{n_{i+1,\hat{i}+1}} \\ \mathbf{0}_{n_{i-1,\hat{i}-1}} & -\hat{I}_{i,\hat{i}+1} & \hat{I}_{i+1,\hat{i}} \end{pmatrix} & \text{otherwise} \end{cases}$$

and $\tilde{I}_i = \text{diag}(\gamma_{i,k}^{\hat{i}-1} I_{n_{i-1} + \lfloor 0.5n_i \rfloor}, \gamma_{i,k}^{\hat{i}+1} I_{n_i - \lfloor 0.5n_i \rfloor + n_{i+1}})$. Further define

$$\tilde{H}_i = \begin{cases} \hat{I}_{i,\hat{i}+1}, & \text{if } i = 1 \\ \hat{I}_{i,\hat{i}-1}, & \text{if } i = n \\ \begin{pmatrix} \hat{I}_{i,\hat{i}-1} & \hat{I}_{i,\hat{i}+1} \end{pmatrix} & \text{otherwise.} \end{cases}$$

The third term in (17) is equivalent to

$$\begin{aligned} & \sum_{i=1}^N \left(\sum_{j \in \mathcal{N}_i} \tilde{I}_{i,j}^T \gamma_{i,k}^j \mathbf{w}_{i,k}^j \right)^T G_{i,k} \left(\sum_{j \in \mathcal{N}_i} \tilde{I}_{i,j}^T \gamma_{i,k}^j \mathbf{w}_{i,k}^j \right) \\ &= \sum_{i=1}^N \boldsymbol{\eta}_{\mathcal{J}_i, k|k-1}^T \tilde{L}_i \tilde{L}_i^T \tilde{H}_i^T G_{i,k} \tilde{H}_i \tilde{L}_i \boldsymbol{\eta}_{\mathcal{J}_i, k|k-1} \\ &\leq \sum_{i=1}^N (\gamma_{i,k}^{\max})^2 \lambda_{\max} \left(\tilde{L}_i^T \tilde{H}_i^T G_{i,k} \tilde{H}_i \tilde{L}_i \right) \|\boldsymbol{\eta}_{\mathcal{J}_i, k|k-1}\|^2 \end{aligned}$$

where $\gamma_{i,k}^{\max} = \max_{j \in \mathcal{N}_i} \gamma_{i,k}^j$ and λ_{\max} (resp. λ_{\min}) is the maximum (resp. minimum) eigenvalue of a matrix.

Step 4: The negative definiteness of (17).

Given Step 1, the first term of (17) can be equivalently written as

$$\begin{aligned} & \sum_{i=1}^N -\boldsymbol{\eta}_{i, k|k-1}^T \Lambda_{i, k-1} \boldsymbol{\eta}_{i, k|k-1} \\ &= \sum_{i=1}^N -\boldsymbol{\eta}_{\mathcal{J}_i, k|k-1}^T \Lambda_{\mathcal{J}_i, k-1} \boldsymbol{\eta}_{\mathcal{J}_i, k|k-1} \end{aligned}$$

where $\Lambda_{\mathcal{J}_i, k} = \text{diag}_{j \in \mathcal{J}_i} (\mu_j^i \Lambda_{j, k})$ with the indexes j sorted by ascending order, and the scaling factors are predefined and satisfy $\sum_{j \in \mathcal{J}_i} \mu_j^i = 1$ for all i . Given Steps 1–3, ΔV_k satisfies

$$\begin{aligned} \Delta V_k &\leq -2 \sum_{i=1}^{N-1} \gamma_{i,k}^{\hat{i}+1} \hat{\boldsymbol{\eta}}_{i, k|k-1}^T \hat{L}_i \hat{\boldsymbol{\eta}}_{i, k|k-1} \\ &+ \sum_{i=1}^N \left((\gamma_{i,k}^{\max})^2 \lambda_{\max} \left(\tilde{L}_i^T \tilde{H}_i^T G_{i,k} \tilde{H}_i \tilde{L}_i \right) \right. \\ &\quad \left. - \lambda_{\min} (\Lambda_{\mathcal{J}_i, k-1}) \right) \|\boldsymbol{\eta}_{\mathcal{J}_i, k|k-1}\|^2. \end{aligned} \quad (20)$$

Therefore, by choosing $\gamma_{i,k}^j$ sufficiently small we can render $\Delta V_k < 0$ for all $k \geq 0$ and for all $\boldsymbol{\eta}_{1:N, k-1|k-1} \neq 0$. Precisely, we need $\gamma_{i,k}^j < \gamma_{i,k}^*$ where $\gamma_{i,k}^*$ is defined by

$$\gamma_{i,k}^* = \left(\frac{\lambda_{\min} (\Lambda_{\mathcal{J}_i, k-1})}{\lambda_{\max} \left(\tilde{L}_i^T \tilde{H}_i^T G_{i,k} \tilde{H}_i \tilde{L}_i \right)} \right)^{\frac{1}{2}}.$$

Note that to compute $\gamma_{i,k}^*$, only information from one-hop neighbors is needed, and global communication topology is not required compared to [4]. Hence, $\Delta V_k < 0$ for all $k \geq 0$ and $\boldsymbol{\eta}_{1:N, k-1|k-1} \neq 0$, and therefore $\boldsymbol{\eta}_{1:N, k|k} = 0$ is GAS for the mean error dynamics of the DLKCF. Consequently, all estimators reach consensus on the shared states. ■

When the consensus gain is zero, the mean error dynamics of each local agent is also GAS under observable modes. However, due to different model errors and innovation sequences, the estimates provided by neighboring agents on their shared overlapping regions inevitably disagree in any realization of the

filter. Hence, the consensus term is designed to promote agreement without destabilizing the filter, which is further verified in Section V-A. Moreover, when $\gamma_{i,k}^j < \gamma_{i,k}^*$, it can be deduced from (20) that $\Delta V_k < -\sqrt{2} \sum_{i=1}^{N-1} \gamma_{i,k}^{\hat{i}+1} \|\mathbf{u}_{i,k}^{\hat{i}+1}\|^2$ (derived in the arXiv version of this work [23, Appendix E]). This indicates that V_k strictly decreases at the rate proportional to the total disagreement until the neighboring disagreements on all the overlapping regions converge to zero, which is a property cannot be achieved without the consensus term.

B. Ultimately Bounded Mean Estimates in Unobservable Modes

Challenges for estimating an unobservable section stem from the dependence of the system dynamics of the SMM on the shock velocity and location, which are functions of the state variables to be estimated. Hence, nonobservability of the system will lead to unknown system dynamics. Moreover, the unobservable modes are also undetectable since the density of the cells in the unobservable subsystem does not dissipate. In this section, we show that the mean estimates of all the cells in an unobservable section are ultimately bounded inside $[-\epsilon, \varrho_m + \epsilon]$ for all $\epsilon > 0$, provided that the upstream and downstream measurements are available. This ensures that the mean estimates of the DLKCF for unobservable modes are always physically meaningful to within ϵ . Since this section studies the properties of the filter for an individual unobservable freeway section, the section index i is dropped for notational simplicity.

Let $[k_U, \bar{k}_U]$ be the time interval² inside which a section switches among unobservable modes, i.e., the mode index $\sigma(k) \in \{\text{FC1}, \text{FC2}\}$ for $k \in [k_U, \bar{k}_U]$, and $\sigma(k) \in \{\text{FF}, \text{CC}, \text{CF}\}$ for $k = k_U$ and $k = \bar{k}_U + 1$. First, we present a lemma stating the boundedness of the Kalman gain for $k \in [k_U, \bar{k}_U]$, which is necessary for showing the boundedness of the state estimate.

Lemma 2: Consider a freeway section that switches among the unobservable modes while $k \in [k_U, \bar{k}_U]$, where $0 \leq k_U < \bar{k}_U \leq +\infty$. Given density measurements of the boundary cells, the Kalman gain computed by the DLKCF (10) and (11) satisfies

$$\|K_k\|_{\infty} \leq \mathfrak{k}(\Gamma_{k_U|k_U}), \quad \text{for all } k \in [k_U, \bar{k}_U] \quad (21)$$

where $\mathfrak{k}(\cdot)$ is a function of the error covariance at time k_U .

Proof: The bound for $\|K_k\|_{\infty}$ is derived in Lemma 4.6 of the arXiv version of this work [23]. ■

Proposition 2: Consider an unobservable section in a road network with dimension n . For all $\epsilon > 0$, a finite time $T(\epsilon)$ exists such that $\boldsymbol{\rho}_{k|k}^l \in [-\epsilon, \varrho_m + \epsilon]$ for all $k > T(\epsilon)$ and for all $l \in \{1, \dots, n\}$, independent of the initial estimate.

Proof: The proof is reported in [19, Proposition 2]. ■

Proposition 2 indicates that when the estimation error of the boundary cells converges to zero, it will drive the state estimate of the interior cells inside $[0, \varrho_m]$ due to the conservation law and the flow-density relationship embedded in the traffic

²The time instant $k \in \mathbb{N}$ throughout this paper. Hence, $k \in [k_U, \bar{k}_U]$ means $k \in \{k_U + 1, \dots, \bar{k}_U\}$.

model. Hence, it is necessary to ensure the error dynamics of the boundary cells is asymptotically stable.

C. Boundedness of the Mean Error Under Switches Among Observable and Unobservable Modes

This section derives the upper bound for the 2-norm of the mean estimation error when a freeway section switches among observable and unobservable modes. We first analyze the upper bound of the mean error when the section switches among the unobservable modes, which quantifies the increase of the mean error while the section is unobservable. Next, the convergence rate of the mean error dynamics while the section switches among the observable modes is studied. Finally, we derive the minimum number of time steps (i.e., the residence time) required in observable modes to ensure the boundedness of the mean error. All results in this section hold for every individual freeway section. In the analysis below, we drop the section index i when it can be omitted for notational simplicity.

1) Upper Bound of the Mean Error in Unobservable Modes: For a freeway section that switches among the unobservable modes while $k \in (\underline{k}_U, \bar{k}_U]$, the next proposition applies Lemma 2 to derive an upper bound for $\|\boldsymbol{\eta}_{k|k}\|$, which is uniform across all $k \in (\underline{k}_U, \bar{k}_U]$. The derived bound is a function of ϵ (ϵ is defined as the upper bound for $\|\boldsymbol{\eta}_{\underline{k}_U|\underline{k}_U}\|$) and $\Gamma_{\underline{k}_U|\underline{k}_U}$, and is larger than ϵ . Moreover, the derived bound does not depend on the length of time interval $(\underline{k}_U, \bar{k}_U]$.

Proposition 3: Consider a freeway section that switches among the unobservable modes while $k \in (\underline{k}_U, \bar{k}_U]$, where $0 \leq \underline{k}_U < \bar{k}_U \leq +\infty$. Let

$$c_0 = \max \left\{ 1, \sqrt{\check{c}_2 \check{c}_1^{-1} r_2 q_1^{-1}} \right\}$$

$$\mathfrak{c}(\Gamma_{\underline{k}_U|\underline{k}_U}) = c_0 \Delta x \mathfrak{k}(\Gamma_{\underline{k}_U|\underline{k}_U}) (\Delta t \min \{v_m, w\})^{-1} \quad (22)$$

where $\check{c}_1 = \check{a}(1 + \check{a}\check{b})^{-1}$ and $\check{c}_2 = \check{a}^{-1}(1 + \check{a}\check{b})$, with $\check{a} = \min \{2r_2^{-1}, q_1\}$ and $\check{b} = \max \{2r_1^{-1}, q_2\}$, and $\mathfrak{k}(\cdot)$ is given in (21). For all $\epsilon > 0$, if $\|\boldsymbol{\eta}_{\underline{k}_U|\underline{k}_U}\| < \epsilon$, then $\|\boldsymbol{\eta}_{k|k}\| < \mathfrak{h}(\epsilon, \Gamma_{\underline{k}_U|\underline{k}_U})$ for all $k \in (\underline{k}_U, \bar{k}_U]$, where $\mathfrak{h}(\epsilon, \Gamma_{\underline{k}_U|\underline{k}_U}) = \sqrt{n}(\varrho_m + \epsilon(\mathfrak{c}(\Gamma_{\underline{k}_U|\underline{k}_U)) + (n-2)\mathfrak{c}(\Gamma_{\underline{k}_U|\underline{k}_U}))$.

Proof: The proof is by induction.

Step 1 : Denote as $\check{\boldsymbol{\eta}}_{k|k}^{(1)} = (\boldsymbol{\eta}_{k|k}^1, \boldsymbol{\eta}_{k|k}^n)^T$ the mean error of the observable subsystem³ (i.e., the boundary cells). The error covariance of the observable subsystem $\check{\Gamma}_{k|k}^{(1)}$ satisfies

$$\check{\Gamma}_{k|k}^{(1)} < r_2 I, \quad \text{and} \quad \check{\Gamma}_{k|k-1}^{(1)} > q_1 I, \quad \text{for } k \in (\underline{k}_U, \bar{k}_U].$$

Let $\check{A}^{(1)} = I$ be the state transition matrix associated with the observable subsystem, it follows that

$$\begin{aligned} \left\| \check{\boldsymbol{\eta}}_{\underline{k}_U+1|\underline{k}_U+1}^{(1)} \right\| &\leq \left\| \left(I - \check{K}_{\underline{k}_U+1}^{(1)} \check{H}^{(1)} \right) \check{A}^{(1)} \right\| \left\| \check{\boldsymbol{\eta}}_{\underline{k}_U|\underline{k}_U}^{(1)} \right\| \\ &= \left\| \check{\Gamma}_{\underline{k}_U+1|\underline{k}_U+1}^{(1)} \left(\check{\Gamma}_{\underline{k}_U+1|\underline{k}_U}^{(1)} \right)^{-1} \right\| \left\| \check{\boldsymbol{\eta}}_{\underline{k}_U|\underline{k}_U}^{(1)} \right\| < r_2 q_1^{-1} \left\| \check{\boldsymbol{\eta}}_{\underline{k}_U|\underline{k}_U}^{(1)} \right\|. \end{aligned}$$

³A detailed description of the observable and unobservable subsystems is given in the arXiv version [23, Appendix F].

Denote as $\check{\mathcal{I}}_{\cdot}^{(1)}$ and $\check{\mathcal{C}}_{\cdot}^{(1)}$ the information and controllability matrix of the observable subsystem, we have $2r_2^{-1}I < \check{\mathcal{I}}_{k,k-1}^{(1)} = R_{k-1}^{-1} + R_k^{-1} < 2r_1^{-1}I$ and $q_1 I < \check{\mathcal{C}}_{k,k-1}^{(1)} = \check{Q}_k^{(1)} < q_2 I$ for all $k \in (\underline{k}_U, \bar{k}_U]$, where $\check{Q}_k^{(1)}$ is the model error covariance for the observable subsystem. Hence, $\check{c}_1 I < (\check{\Gamma}_{k|k}^{(1)})^{-1} < \check{c}_2 I$ for all $k \in (\underline{k}_U, \bar{k}_U]$ according to [26, Lemma 7.1 and 7.2]. Define the Lyapunov function of the observable subsystem as $\check{V}_k = (\check{\boldsymbol{\eta}}_{k|k}^{(1)})^T (\check{\Gamma}_{k|k}^{(1)})^{-1} \check{\boldsymbol{\eta}}_{k|k}^{(1)}$, then $\check{V}_{k+1} < \check{V}_k$ for all $k \in (\underline{k}_U, \bar{k}_U]$ due to [4, Lemma 3]. Consequently

$$\left\| \check{\boldsymbol{\eta}}_{k|k}^{(1)} \right\| < \left(\frac{\check{V}_k}{\check{c}_1} \right)^{\frac{1}{2}} < \left(\frac{\check{V}_{\underline{k}_U+1}}{\check{c}_1} \right)^{\frac{1}{2}} < \sqrt{\check{c}_2 \check{c}_1^{-1}} \left\| \check{\boldsymbol{\eta}}_{\underline{k}_U+1|\underline{k}_U+1}^{(1)} \right\|$$

for all $k \in (\underline{k}_U + 1, \bar{k}_U]$. It follows that for all $k \in (\underline{k}_U, \bar{k}_U]$:

$$\left\| \check{\boldsymbol{\eta}}_{k|k}^{(1)} \right\| < \sqrt{\check{c}_2 \check{c}_1^{-1} r_2 q_1^{-1}} \left\| \check{\boldsymbol{\eta}}_{\underline{k}_U|\underline{k}_U}^{(1)} \right\| < \sqrt{\check{c}_2 \check{c}_1^{-1} r_2 q_1^{-1}} \epsilon \leq c_0 \epsilon.$$

Step 2: We use induction to show that $\boldsymbol{\rho}_{k|k}^l > -c_0 \epsilon - (l-1)\mathfrak{c}(\Gamma_{\underline{k}_U|\underline{k}_U})\epsilon \geq -\epsilon(c_0 + (n-2)\mathfrak{c}(\Gamma_{\underline{k}_U|\underline{k}_U}))$ for all $k \in (\underline{k}_U, \bar{k}_U]$ and $l \in \{2, \dots, n-1\}$. Since $|\boldsymbol{\eta}_{k|k}^1| < c_0 \epsilon$ for all $k \in (\underline{k}_U, \bar{k}_U]$, it holds that $\boldsymbol{\rho}_{k|k}^1 > -c_0 \epsilon = -c_0 \epsilon - (1-1)\mathfrak{c}(\Gamma_{\underline{k}_U|\underline{k}_U})\epsilon$. Hence when $l=1$, $\boldsymbol{\rho}_{k|k}^1 > -c_0 \epsilon - (l-1)\mathfrak{c}(\Gamma_{\underline{k}_U|\underline{k}_U})\epsilon$ holds for all $k \in (\underline{k}_U, \bar{k}_U]$.

For $l \in \{1, 2, \dots, n-2\}$, suppose $\boldsymbol{\rho}_{k|k}^l > -c_0 \epsilon - (l-1)\mathfrak{c}(\Gamma_{\underline{k}_U|\underline{k}_U})\epsilon$ for all $k \in (\underline{k}_U, \bar{k}_U]$. If $\boldsymbol{\rho}_{k|k}^{l+1} < -c_0 \epsilon - l\mathfrak{c}(\Gamma_{\underline{k}_U|\underline{k}_U})\epsilon$, we obtain from (4) that

$$\begin{aligned} \mathfrak{f}(\boldsymbol{\rho}_{k|k}^l, \boldsymbol{\rho}_{k|k}^{l+1}) &= v_m \boldsymbol{\rho}_{k|k}^l > v_m (-c_0 \epsilon - (l-1)\mathfrak{c}(\Gamma_{\underline{k}_U|\underline{k}_U})\epsilon) \\ \mathfrak{f}(\boldsymbol{\rho}_{k|k}^{l+1}, \boldsymbol{\rho}_{k|k}^{l+2}) &\leq v_m \boldsymbol{\rho}_{k|k}^{l+1}. \end{aligned}$$

It follows that the estimate of cell $l+1$ satisfies:

$$\begin{aligned} \boldsymbol{\rho}_{k+1|k+1}^{l+1} &= \boldsymbol{\rho}_{k|k}^{l+1} + \frac{\Delta t}{\Delta x} \left(\mathfrak{f}(\boldsymbol{\rho}_{k|k}^l, \boldsymbol{\rho}_{k|k}^{l+1}) - \mathfrak{f}(\boldsymbol{\rho}_{k|k}^{l+1}, \boldsymbol{\rho}_{k|k}^{l+2}) \right) \\ &\quad - K_{k+1}(l+1, 1)\boldsymbol{\eta}_{k+1|k}^1 - K_{k+1}(l+1, 2)\boldsymbol{\eta}_{k+1|k}^2 \\ &> \boldsymbol{\rho}_{k|k}^{l+1} + \frac{v_m \Delta t}{\Delta x} \left| \boldsymbol{\rho}_{k|k}^{l+1} + c_0 \epsilon + (l-1)\mathfrak{c}(\Gamma_{\underline{k}_U|\underline{k}_U})\epsilon \right| \\ &\quad - \mathfrak{k}(\Gamma_{\underline{k}_U|\underline{k}_U}) c_0 \epsilon \\ &= \boldsymbol{\rho}_{k|k}^{l+1} + \frac{v_m \Delta t}{\Delta x} \left| \boldsymbol{\rho}_{k|k}^{l+1} + c_0 \epsilon + l\mathfrak{c}(\Gamma_{\underline{k}_U|\underline{k}_U})\epsilon \right| \\ &\quad + \frac{v_m \Delta t}{\Delta x} \mathfrak{c}(\Gamma_{\underline{k}_U|\underline{k}_U})\epsilon - \mathfrak{k}(\Gamma_{\underline{k}_U|\underline{k}_U}) c_0 \epsilon \\ &\geq \boldsymbol{\rho}_{k|k}^{l+1} + \frac{v_m \Delta t}{\Delta x} \left| \boldsymbol{\rho}_{k|k}^{l+1} + c_0 \epsilon + l\mathfrak{c}(\Gamma_{\underline{k}_U|\underline{k}_U})\epsilon \right| \end{aligned}$$

where the first inequality is due to $\|K_k\|_\infty \leq \mathfrak{k}(\Gamma_{\underline{k}_U|\underline{k}_U})$ given in Lemma 2 and the fact that $\|\check{\boldsymbol{\eta}}_{k+1|k}^{(1)}\| = \|\check{A}^{(1)}\check{\boldsymbol{\eta}}_{k|k}^{(1)}\| = \|\check{\boldsymbol{\eta}}_{k|k}^{(1)}\| < c_0 \epsilon$ for all $k \in (\underline{k}_U, \bar{k}_U]$, and the last inequality

is obtained by $\frac{v_m \Delta t}{\Delta x} \mathbf{c}(\Gamma_{\underline{k}_U|\underline{k}_U})\epsilon - \mathbf{f}(\Gamma_{\underline{k}_U|\underline{k}_U})c_0\epsilon = \frac{v_m}{\min\{v_m, w\}} \mathbf{f}(\Gamma_{\underline{k}_U|\underline{k}_U})c_0\epsilon - \mathbf{f}(\Gamma_{\underline{k}_U|\underline{k}_U})c_0\epsilon \geq 0$. Also since $\rho_{\underline{k}_U|\underline{k}_U}^{l+1} > -\epsilon \geq -c_0\epsilon > -c_0\epsilon - lc(\Gamma_{\underline{k}_U|\underline{k}_U})\epsilon$, it is concluded that $\rho_{k|k}^{l+1} > -c_0\epsilon - lc(\Gamma_{\underline{k}_U|\underline{k}_U})\epsilon$ for all $k \in (\underline{k}_U, \bar{k}_U]$. Continuing the induction along the cells, we obtain $\rho_{k|k}^{n-1} > -c_0\epsilon - (n-2)c(\Gamma_{\underline{k}_U|\underline{k}_U})\epsilon$ for all $k \in (\underline{k}_U, \bar{k}_U]$.

We can use a similar induction to show $\rho_{k|k}^l < \varrho_m + c_0\epsilon + (n-l)c(\Gamma_{\underline{k}_U|\underline{k}_U})\epsilon \leq \varrho_m + \epsilon(c_0 + (n-2)c(\Gamma_{\underline{k}_U|\underline{k}_U}))$ for all $k \in (\underline{k}_U, \bar{k}_U]$ and $l \in \{2, \dots, n-1\}$.

Step 3: Combining Steps 1 and 2, we obtain $\rho_{k|k}^l \in (-\epsilon(c_0 + (n-2)c(\Gamma_{\underline{k}_U|\underline{k}_U))), \varrho_m + \epsilon(c_0 + (n-2)c(\Gamma_{\underline{k}_U|\underline{k}_U}))$ for all $l \in \{1, \dots, n\}$ and $k \in (\underline{k}_U, \bar{k}_U]$. Consequently, $\|\boldsymbol{\eta}_{k|k}\| < \sqrt{n}(\varrho_m + \epsilon(c_0 + (n-2)c(\Gamma_{\underline{k}_U|\underline{k}_U)))) = \mathfrak{h}(\epsilon, \Gamma_{\underline{k}_U|\underline{k}_U})$ for all $k \in (\underline{k}_U, \bar{k}_U]$. ■

2) *Convergence Rate of the Mean Error in Observable Modes:* Let $(\underline{k}_O, \bar{k}_O]$ be the time interval inside that a section switches among observable modes, i.e., the mode index $\sigma(k) \in \{\text{FF}, \text{CC}, \text{CF}\}$ for $k \in (\underline{k}_O, \bar{k}_O]$, and $\sigma(k) \in \{\text{FC1}, \text{FC2}\}$ for $k = \underline{k}_O$ and $k = \bar{k}_O + 1$. Due to the boundedness of the consensus term described in (13), the mean error satisfies

$$\|\boldsymbol{\eta}_{k|k}\| \leq \left\| \prod_{\kappa=k-1}^{\underline{k}_O} F_{\kappa+1} A_{\kappa} \right\| \|\boldsymbol{\eta}_{\underline{k}_O|\underline{k}_O}\| + \hat{c} \left(1 + \sum_{\iota=1}^{k-\underline{k}_O-1} \left\| \prod_{\kappa=k-\iota}^{\underline{k}_O} F_{\kappa+1} A_{\kappa} \right\| \right) \quad (23)$$

for $k \in (\underline{k}_O, \bar{k}_O]$, where $F_k = I - K_k H_k$. According to (23), we need to analyze the magnitude of $\left\| \prod_{\kappa=k-1}^{\underline{k}_O} F_{\kappa+1} A_{\kappa} \right\|$ in order to study the convergence rate of the mean estimation error, which is detailed in the Lemma 3.

Lemma 3: Consider a freeway section that switches among the observable modes while $k \in (\underline{k}_O, \bar{k}_O]$, where $0 \leq \underline{k}_O < \bar{k}_O \leq +\infty$. If the error covariance satisfies $\mathbf{0} < d_1 I \leq \Gamma_{k|k}^{-1} \leq d_2 I$ for all $\underline{k}_O < k \leq \bar{k}_O$, where $d_1, d_2 \in \mathbb{R}^+$, then

$$\left\| \prod_{\kappa=k-1}^{\underline{k}_O} F_{\kappa+1} A_{\kappa} \right\| \leq \hat{a} \hat{q}^{k-\underline{k}_O}, \quad \text{for } k \in (\underline{k}_O, \bar{k}_O] \quad (24)$$

where $\hat{a} = (d_2 d_1^{-1})^{\frac{1}{2}} \geq 1$, $0 < \hat{q} = (1 - \mathfrak{d}(d_1, d_2) d_2^{-1})^{\frac{1}{2}} < 1$, and $\mathfrak{d}(\cdot, \cdot)$ is a function of d_1, d_2 defined by

$$\mathfrak{d}(d_1, d_2) = \left(d_1^{-1} + q_1^{-1} d_1^{-2} \max_{M \in \mathcal{A}_O} \sigma_{\max}^2(M) \right)^{-1}$$

where $\mathcal{A}_O = \{A_{\text{FF}}, A_{\text{CC}}, A_{\text{CF}}^s | s \in \{1, 2, \dots, n-1\}\}$ and $\sigma_{\max}(M)$ is the maximum singular value of matrix M .

Proof: See the arXiv version of this work [23, Appendix I]. ■

3) *Residence Time in Observable Modes:* When a freeway section switches from an unobservable mode at time \underline{k}_O to an observable mode at $\underline{k}_O + 1$, the next proposition derives

the residence time the section must remain in the set of observable modes in order to reduce the mean estimation error below a given threshold. The residence time is a function of the mean error and error covariance of the section at time \underline{k}_O , and also depends on the magnitude of the mean error to be satisfied.

Proposition 4: Consider a freeway section that switches among the observable modes while $k \in (\underline{k}_O, \bar{k}_O]$, where $0 \leq \underline{k}_O < \bar{k}_O \leq +\infty$. Define

$$\begin{aligned} \mathbf{a}(\Gamma_{\underline{k}_O|\underline{k}_O}) &= \left(\mathbf{c}_2(\Gamma_{\underline{k}_O|\underline{k}_O}) (\mathbf{c}_1(\Gamma_{\underline{k}_O|\underline{k}_O}))^{-1} \right)^{\frac{1}{2}} \\ \mathbf{q}(\Gamma_{\underline{k}_O|\underline{k}_O}) &= \left(1 - \mathbf{c}_3(\Gamma_{\underline{k}_O|\underline{k}_O}) (\mathbf{c}_2(\Gamma_{\underline{k}_O|\underline{k}_O}))^{-1} \right)^{\frac{1}{2}} \end{aligned} \quad (25)$$

where $\mathbf{c}_1(\cdot)$, $\mathbf{c}_2(\cdot)$ are the bounds from (18), and $\mathbf{c}_3(\Gamma_{\underline{k}_O|\underline{k}_O})$ is given by $\mathbf{c}_3(\Gamma_{\underline{k}_O|\underline{k}_O}) = \mathfrak{d}(\mathbf{c}_1(\Gamma_{\underline{k}_O|\underline{k}_O}), \mathbf{c}_2(\Gamma_{\underline{k}_O|\underline{k}_O}))$ with $\mathfrak{d}(\cdot, \cdot)$ defined in Lemma 3.

For all $\epsilon > 0$, there exists $\mathfrak{t}(\epsilon, \|\boldsymbol{\eta}_{\underline{k}_O|\underline{k}_O}\|, \Gamma_{\underline{k}_O|\underline{k}_O})$ such that if $\bar{k}_O - \underline{k}_O > \mathfrak{t}(\epsilon, \|\boldsymbol{\eta}_{\underline{k}_O|\underline{k}_O}\|, \Gamma_{\underline{k}_O|\underline{k}_O})$, the mean error at time \bar{k}_O satisfies $\|\boldsymbol{\eta}_{\bar{k}_O|\bar{k}_O}\| < \epsilon + \hat{c} + \frac{\hat{c} \mathbf{a}(\Gamma_{\underline{k}_O|\underline{k}_O}) \mathbf{q}(\Gamma_{\underline{k}_O|\underline{k}_O})}{1 - \mathbf{q}(\Gamma_{\underline{k}_O|\underline{k}_O})}$. Explicitly

$$\begin{aligned} \mathfrak{t}(\epsilon, \|\boldsymbol{\eta}_{\underline{k}_O|\underline{k}_O}\|, \Gamma_{\underline{k}_O|\underline{k}_O}) &= \\ &\begin{cases} 0, & \text{if } \mathbf{a}(\Gamma_{\underline{k}_O|\underline{k}_O}) \mathbf{q}(\Gamma_{\underline{k}_O|\underline{k}_O}) \|\boldsymbol{\eta}_{\underline{k}_O|\underline{k}_O}\| \leq \frac{\hat{c} \mathbf{a}(\Gamma_{\underline{k}_O|\underline{k}_O}) \mathbf{q}(\Gamma_{\underline{k}_O|\underline{k}_O})}{1 - \mathbf{q}(\Gamma_{\underline{k}_O|\underline{k}_O})} \\ \log_{\mathbf{q}(\Gamma_{\underline{k}_O|\underline{k}_O})} \left(\epsilon \left(\mathbf{a}(\Gamma_{\underline{k}_O|\underline{k}_O}) \|\boldsymbol{\eta}_{\underline{k}_O|\underline{k}_O}\| - \frac{\hat{c} \mathbf{a}(\Gamma_{\underline{k}_O|\underline{k}_O}) \mathbf{q}(\Gamma_{\underline{k}_O|\underline{k}_O})}{1 - \mathbf{q}(\Gamma_{\underline{k}_O|\underline{k}_O})} \right)^{-1} \right) & \text{otherwise.} \end{cases} \end{aligned} \quad (26)$$

Furthermore, for all $k \in (\underline{k}_O, \bar{k}_O]$

$$\begin{aligned} \|\boldsymbol{\eta}_{k|k}\| &\leq \max \left\{ \hat{c} + \mathbf{a}(\Gamma_{\underline{k}_O|\underline{k}_O}) \mathbf{q}(\Gamma_{\underline{k}_O|\underline{k}_O}) \|\boldsymbol{\eta}_{\underline{k}_O|\underline{k}_O}\|, \right. \\ &\quad \left. \hat{c} + \hat{c} \mathbf{a}(\Gamma_{\underline{k}_O|\underline{k}_O}) \mathbf{q}(\Gamma_{\underline{k}_O|\underline{k}_O}) (1 - \mathbf{q}(\Gamma_{\underline{k}_O|\underline{k}_O)))^{-1} \right\}. \end{aligned}$$

Proof: According to Lemma 1, when $\underline{k}_O < k \leq \bar{k}_O$ the error covariance satisfies $\mathbf{c}_1(\Gamma_{\underline{k}_O|\underline{k}_O}) I \leq \Gamma_{k|k}^{-1} \leq \mathbf{c}_2(\Gamma_{\underline{k}_O|\underline{k}_O}) I$. Given Lemma 3, it follows that for $\underline{k}_O < k \leq \bar{k}_O$:

$$\left\| \prod_{\kappa=k-1}^{\underline{k}_O} F_{\kappa+1} A_{\kappa} \right\| \leq \mathbf{a}(\Gamma_{\underline{k}_O|\underline{k}_O}) \mathbf{q}(\Gamma_{\underline{k}_O|\underline{k}_O})^{k-\underline{k}_O}$$

where $\mathbf{a}(\Gamma_{\underline{k}_O|\underline{k}_O}) \geq 1$ provides an upper bound for the increase of the mean estimation error when the section first switches to an observable mode at time $\underline{k}_O + 1$, and $0 < \mathbf{q}(\Gamma_{\underline{k}_O|\underline{k}_O}) < 1$ describes the convergence rate of the mean estimation error in observable modes. Hence when $\underline{k}_O < k \leq \bar{k}_O$, the 2-norm of

$\boldsymbol{\eta}_{k|k}$ satisfies

$$\begin{aligned}
\|\boldsymbol{\eta}_{k|k}\| &\leq \left\| \prod_{\kappa=k-1}^{\underline{k}_O} F_{\kappa+1} A_{\kappa} \right\| \|\boldsymbol{\eta}_{\underline{k}_O|\underline{k}_O}\| \\
&\quad + \hat{c} \left(1 + \sum_{\iota=1}^{k-\underline{k}_O-1} \left\| \prod_{\kappa=k-1}^{\underline{k}_O+\iota} F_{\kappa+1} A_{\kappa} \right\| \right) \\
&\leq \hat{c} + \|\boldsymbol{\eta}_{\underline{k}_O|\underline{k}_O}\| \mathbf{a}(\Gamma_{\underline{k}_O|\underline{k}_O}) \mathbf{q}(\Gamma_{\underline{k}_O|\underline{k}_O})^{k-\underline{k}_O} \\
&\quad + \sum_{\iota=1}^{k-\underline{k}_O-1} \hat{c} \mathbf{a}(\Gamma_{\underline{k}_O|\underline{k}_O}) \mathbf{q}(\Gamma_{\underline{k}_O|\underline{k}_O})^{k-\underline{k}_O-\iota} \\
&= \hat{c} + \|\boldsymbol{\eta}_{\underline{k}_O|\underline{k}_O}\| \mathbf{a}(\Gamma_{\underline{k}_O|\underline{k}_O}) \mathbf{q}(\Gamma_{\underline{k}_O|\underline{k}_O})^{k-\underline{k}_O} \\
&\quad + \frac{\hat{c} \mathbf{a}(\Gamma_{\underline{k}_O|\underline{k}_O}) \mathbf{q}(\Gamma_{\underline{k}_O|\underline{k}_O})}{1 - \mathbf{q}(\Gamma_{\underline{k}_O|\underline{k}_O})} \left(1 - \mathbf{q}(\Gamma_{\underline{k}_O|\underline{k}_O})^{k-\underline{k}_O-1} \right) \\
&\triangleq \mathbf{u}(\Gamma_{\underline{k}_O|\underline{k}_O}, k)
\end{aligned}$$

where for a fixed $\Gamma_{\underline{k}_O|\underline{k}_O}$, the function $\mathbf{u}(\Gamma_{\underline{k}_O|\underline{k}_O}, k)$ is either nonincreasing or nondecreasing with respect to k . As a consequence, for all $\epsilon > 0$, there exists $\mathbf{t}(\epsilon, \|\boldsymbol{\eta}_{\underline{k}_O|\underline{k}_O}\|, \Gamma_{\underline{k}_O|\underline{k}_O}) \geq 0$ such that for all $k - \underline{k}_O > \mathbf{t}(\epsilon, \|\boldsymbol{\eta}_{\underline{k}_O|\underline{k}_O}\|, \Gamma_{\underline{k}_O|\underline{k}_O})$

$$\|\boldsymbol{\eta}_{k|k}\| < \epsilon + \hat{c} + \frac{\hat{c} \mathbf{a}(\Gamma_{\underline{k}_O|\underline{k}_O}) \mathbf{q}(\Gamma_{\underline{k}_O|\underline{k}_O})}{1 - \mathbf{q}(\Gamma_{\underline{k}_O|\underline{k}_O})}.$$

When $\mathbf{a}(\Gamma_{\underline{k}_O|\underline{k}_O}) \mathbf{q}(\Gamma_{\underline{k}_O|\underline{k}_O}) \|\boldsymbol{\eta}_{\underline{k}_O|\underline{k}_O}\| \leq \frac{\hat{c} \mathbf{a}(\Gamma_{\underline{k}_O|\underline{k}_O}) \mathbf{q}(\Gamma_{\underline{k}_O|\underline{k}_O})}{1 - \mathbf{q}(\Gamma_{\underline{k}_O|\underline{k}_O})}$, we have $\mathbf{u}(\Gamma_{\underline{k}_O|\underline{k}_O}, \underline{k}_O + 1) \leq \lim_{k \rightarrow \infty} \mathbf{u}(\Gamma_{\underline{k}_O|\underline{k}_O}, k)$, and $\mathbf{u}(\Gamma_{\underline{k}_O|\underline{k}_O}, k) \leq \lim_{k \rightarrow \infty} \mathbf{u}(\Gamma_{\underline{k}_O|\underline{k}_O}, k)$ nondecreasing with respect to $k \in (\underline{k}_O, \bar{k}_O]$, thus $\mathbf{t}(\epsilon, \|\boldsymbol{\eta}_{\underline{k}_O|\underline{k}_O}\|, \Gamma_{\underline{k}_O|\underline{k}_O}) = 0$. On the other hand, $\mathbf{u}(\Gamma_{\underline{k}_O|\underline{k}_O}, k)$ is nonincreasing with respect to k when $\mathbf{u}(\Gamma_{\underline{k}_O|\underline{k}_O}, \underline{k}_O + 1) > \lim_{k \rightarrow \infty} \mathbf{u}(\Gamma_{\underline{k}_O|\underline{k}_O}, k)$. In this case

$$\begin{aligned}
&\mathbf{t}(\epsilon, \|\boldsymbol{\eta}_{\underline{k}_O|\underline{k}_O}\|, \Gamma_{\underline{k}_O|\underline{k}_O}) = \\
&\log_{\mathbf{q}(\Gamma_{\underline{k}_O|\underline{k}_O})} \left(\epsilon \left(\mathbf{a}(\Gamma_{\underline{k}_O|\underline{k}_O}) \|\boldsymbol{\eta}_{\underline{k}_O|\underline{k}_O}\| - \frac{\hat{c} \mathbf{a}(\Gamma_{\underline{k}_O|\underline{k}_O}) \mathbf{q}(\Gamma_{\underline{k}_O|\underline{k}_O})}{1 - \mathbf{q}(\Gamma_{\underline{k}_O|\underline{k}_O})} \right)^{-1} \right).
\end{aligned}$$

Furthermore, the upper bound of $\|\boldsymbol{\eta}_{k|k}\|$ is given as follows:

$$\begin{aligned}
\|\boldsymbol{\eta}_{k|k}\| &\leq \max \left\{ \mathbf{u}(\Gamma_{\underline{k}_O|\underline{k}_O}, \underline{k}_O + 1), \lim_{k \rightarrow \infty} \mathbf{u}(\Gamma_{\underline{k}_O|\underline{k}_O}, k) \right\} \\
&= \max \left\{ \hat{c} + \mathbf{a}(\Gamma_{\underline{k}_O|\underline{k}_O}) \mathbf{q}(\Gamma_{\underline{k}_O|\underline{k}_O}) \|\boldsymbol{\eta}_{\underline{k}_O|\underline{k}_O}\|, \right. \\
&\quad \left. \hat{c} + \frac{\hat{c} \mathbf{a}(\Gamma_{\underline{k}_O|\underline{k}_O}) \mathbf{q}(\Gamma_{\underline{k}_O|\underline{k}_O})}{1 - \mathbf{q}(\Gamma_{\underline{k}_O|\underline{k}_O})} \right\}
\end{aligned}$$

for all $k \in (\underline{k}_O, \bar{k}_O]$, which concludes the proof. \blacksquare

4) *Boundedness of the Mean Estimation Error Under Switches Among Observable and Unobservable Modes:* Based on Proposition 3 and Proposition 4, the boundedness of the mean

estimation error when the SMM switches among observable and unobservable modes is summarized in Proposition 5.

The main concept of Proposition 5 is given as follows. For a freeway section, denote $(\underline{k}_U^r, \bar{k}_U^r]$ and $(\underline{k}_O^r, \bar{k}_O^r]$ as the r th unobservable and observable time intervals, respectively. Consider a freeway section that switches from an observable mode at $\bar{k}_O^{r-1} = \underline{k}_U^r$ to an unobservable mode at $\underline{k}_U^r + 1$, and remains unobservable through \bar{k}_U^r . An upper bound for the 2-norm of the mean estimation error, which is uniform over $(\underline{k}_U^r, \bar{k}_U^r]$, can be obtained through Proposition 3 based on the error covariance and the upper bound of the mean error at time \underline{k}_U^r . When the section switches back to the set of observable modes at time $\bar{k}_U^r + 1 = \underline{k}_O^r + 1$ and remains observable through \bar{k}_O^r , the mean estimation error has been increased during the unobservable time interval, and may continue to increase initially before decreasing while the section is observable. Based on Proposition 4, the minimum residence time $\bar{k}_O^r - \underline{k}_O^r$ the section must remain observable to offset the increase of the mean estimation error, as well as the upper bound of the mean error during the observable interval $(\underline{k}_O^r, \bar{k}_O^r]$ are derived. The minimum residence time ensures that when the section switches back to an unobservable mode, the mean estimation error is smaller than a given upper bound. Based on this upper bound and the error covariance at time $\bar{k}_O^r = \underline{k}_U^{r+1}$, we can apply Proposition 3 again and obtain the upper bound for the 2-norm of the mean estimation error during the unobservable time interval starting at time $\underline{k}_U^{r+1} + 1$. We continue the induction and derive the minimum residence time for each observable time interval, as well as the upper bounds of the 2-norm of the mean estimation error for all the observable and unobservable time intervals.

Proposition 5: For a freeway section, denote $(\underline{k}_U^r, \bar{k}_U^r]$ (resp. $(\underline{k}_O^r, \bar{k}_O^r]$) as the r th time interval while the section switches among unobservable (resp. observable) modes. Hence, $\underline{k}_U^1 = 0$ (resp. $\underline{k}_O^1 = 0$) when the section is unobservable (resp. observable) at time 0. Let $\delta > 0$ be an arbitrary positive constant, and suppose the following conditions on the residence time for the observable time intervals hold

$$\begin{aligned}
&\bar{k}_O^r - \underline{k}_O^r > \\
&\begin{cases} \mathbf{t}(\delta, \mathbf{e}(\delta, \Gamma_{\underline{k}_O^{r-1}|\underline{k}_O^{r-1}}, \Gamma_{\bar{k}_O^{r-1}|\bar{k}_O^{r-1}}), \Gamma_{\underline{k}_O^r|\underline{k}_O^r}) & r \geq 2 \\ \mathbf{t}(\delta, \mathbf{e}_0(\Gamma_{0|0}), \Gamma_{\underline{k}_O^1|\underline{k}_O^1}) & r = 1 \text{ and } \underline{k}_U^1 = 0 \\ \mathbf{t}(\delta, \sqrt{n} \varrho_m, \Gamma_{0|0}) & r = 1 \text{ and } \underline{k}_O^1 = 0 \end{cases}
\end{aligned}$$

where $\mathbf{e}_0(M) = \sqrt{n}(\sqrt{n} \varrho_m (c_0 + (n-2) \mathbf{c}(M)) + \varrho_m)$ for $M \in \mathbb{R}^{n \times n}$, and

$$\begin{aligned}
\mathbf{e}(\delta, M_1, M_2) &= \sqrt{n} \left(\varrho_m + \left(\delta + \hat{c} + \frac{\hat{c} \mathbf{a}(M_1) \mathbf{q}(M_1)}{1 - \mathbf{q}(M_1)} \right) \right. \\
&\quad \left. \times (c_0 + (n-2) \mathbf{c}(M_2)) \right),
\end{aligned}$$

for $M_1, M_2 \in \mathbb{R}^{n \times n}$, with \hat{c} given in (13), c_0 and $\mathbf{c}(\cdot)$ defined in (22), $\mathbf{a}(\cdot)$ and $\mathbf{q}(\cdot)$ defined in (25).

When $r \geq 2$, the mean error is upper bounded as follows:

$$\|\boldsymbol{\eta}_{k|k}\| \leq \begin{cases} (a) \text{ for } k \in (\underline{k}_U^r, \bar{k}_U^r]: \boldsymbol{\epsilon} \left(\delta, \Gamma_{\bar{k}_U^{r-1} | \bar{k}_U^{r-1}}, \Gamma_{\underline{k}_U^r | \underline{k}_U^r} \right) \\ (b) \text{ for } k \in (\underline{k}_O^r, \bar{k}_O^r]: \max \left\{ \hat{c} + \boldsymbol{\alpha} \left(\Gamma_{\underline{k}_O^r | \underline{k}_O^r} \right) \right. \\ \quad \times \boldsymbol{q} \left(\Gamma_{\underline{k}_O^r | \underline{k}_O^r} \right) \boldsymbol{\epsilon} \left(\delta, \Gamma_{\underline{k}_O^{r-1} | \underline{k}_O^{r-1}}, \Gamma_{\bar{k}_O^{r-1} | \bar{k}_O^{r-1}} \right), \\ \quad \hat{c} + \hat{c}\boldsymbol{\alpha} \left(\Gamma_{\underline{k}_O^r | \underline{k}_O^r} \right) \\ \quad \left. \times \boldsymbol{q} \left(\Gamma_{\underline{k}_O^r | \underline{k}_O^r} \right) \left(1 - \boldsymbol{q} \left(\Gamma_{\underline{k}_O^r | \underline{k}_O^r} \right) \right)^{-1} \right\}. \end{cases}$$

When $r = 1$ and $\underline{k}_U^1 = 0$, the mean estimation error satisfies

$$\|\boldsymbol{\eta}_{k|k}\| \leq \begin{cases} (a) \text{ for } k \in (\underline{k}_U^1, \bar{k}_U^1]: \boldsymbol{\epsilon}_0 \left(\Gamma_{0|0} \right) \\ (b) \text{ for } k \in (\underline{k}_O^1, \bar{k}_O^1]: \max \left\{ \hat{c} + \boldsymbol{\alpha} \left(\Gamma_{\underline{k}_O^1 | \underline{k}_O^1} \right) \right. \\ \quad \times \boldsymbol{q} \left(\Gamma_{\underline{k}_O^1 | \underline{k}_O^1} \right) \boldsymbol{\epsilon}_0 \left(\Gamma_{0|0} \right), \hat{c} + \hat{c}\boldsymbol{\alpha} \left(\Gamma_{\underline{k}_O^1 | \underline{k}_O^1} \right) \\ \quad \left. \times \boldsymbol{q} \left(\Gamma_{\underline{k}_O^1 | \underline{k}_O^1} \right) \left(1 - \boldsymbol{q} \left(\Gamma_{\underline{k}_O^1 | \underline{k}_O^1} \right) \right)^{-1} \right\}. \end{cases}$$

When $r = 1$ and $\underline{k}_O^1 = 0$, the mean estimation error satisfies

$$\|\boldsymbol{\eta}_{k|k}\| \leq \begin{cases} (a) \text{ for } k \in (\underline{k}_U^1, \bar{k}_U^1]: \boldsymbol{\epsilon} \left(\delta, \Gamma_{0|0}, \Gamma_{\underline{k}_U^1 | \underline{k}_U^1} \right), \\ (b) \text{ for } k \in (\underline{k}_O^1, \bar{k}_O^1]: \max \left\{ \hat{c} + \boldsymbol{\alpha} \left(\Gamma_{0|0} \right) \right. \\ \quad \times \boldsymbol{q} \left(\Gamma_{0|0} \right) \sqrt{n} \boldsymbol{q}_m, \hat{c} + \hat{c}\boldsymbol{\alpha} \left(\Gamma_{0|0} \right) \\ \quad \left. \times \boldsymbol{q} \left(\Gamma_{0|0} \right) \left(1 - \boldsymbol{q} \left(\Gamma_{0|0} \right) \right)^{-1} \right\}. \end{cases}$$

Proof: The proof is reported in the arXiv version of this work [23]. ■

Remark 2: The minimum residence time in Proposition 5 shares a similar concept with the definition of (average) dwell time (e.g., [27], [28]): both impose conditions on sufficiently long time spent in modes that are GAS (or observable in our case). However, different from the analysis using dwell time, in this work there is no requirement regarding the ratio between the total time spent in observable and unobservable modes, and the minimum residence time here is computed online.

V. NUMERICAL EXPERIMENTS

A. Effect of Interagent Communication and Filter Consistency

In this section, we show the effect of the consensus term in reducing neighbor disagreement, and validate the consistency of the DLKCF using the NEES measure. The network is a stretch of highway divided into 136 cells and seven sections. We apply normalized parameters for the triangular fundamental diagram. The true solution is a combination of an expansion fan and a shock propagating upstream, with a sinusoidal upstream boundary condition [see Fig. 1(a)], which is computed based on the CTM. Elements of the experimental setup not detailed here can be found in the README documentation for the supplementary source code <https://github.com/yesun/DLKCF>.

Disagreement and error on state estimates can be generated for various reasons, here we consider the combining effects

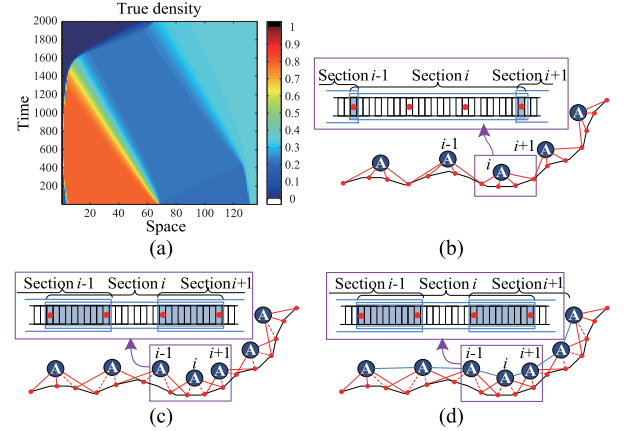


Fig. 1. (a) True Solution; (b)–(d) Freeway network setup and communication topology for: (b) the LKF; (c) the DLKCF-0; and (d) the DLKCF. The red solid lines represent the direct connection between agents (labeled A in circles) and sensors (red dots), and the red dashed lines represent connection between agents and sensors obtained through receiving shared measurements and sensor models from neighbors. The blue lines stand for the existence of consensus terms between agents. In the zoomed-in parts, the freeway is discretized by cells (small rectangles) and localized by sections (blocks). Overlapping regions are represented by the blue shaded cells, and sensor locations are represented by red dots in the cells.

of the following two causes: 1) *heterogeneous sensors* (HS), with some of the sensors having large measurement errors; and 2) *inconsistent agents* (IA), with some agents assuming incorrect (too small) noise models for the low-quality sensors. In this experiment, we put a large-error sensor once every three sensors starting from the downstream sensor of the first section. Moreover, agents associated with sections indexed by even numbers are unable to recognize the large-error sensors they are directly connected to. We also apply perturbations of 10–20% on the model parameters (i.e., \boldsymbol{q}_m , \boldsymbol{q}_c , and \boldsymbol{v}_m).

We explore the following effects of the above two causes on the disagreement and error of estimates.

- 1) The LKF where each local agent runs the KF described in Section III-A independently based on measurements from the sensors it is directly connected to (e.g., $z_{i,k}^j$ for agent i), without sharing measurements or estimates.
- 2) The *DLKCF with zero consensus gain* (DLKCF-0), where the prediction and correction steps are given by (10) and (11) (i.e., neighboring agents share sensor data and sensor models) with consensus gains set to zero (i.e., $C_{i,k}^j = \mathbf{0}_{n_i, n_{i,j}}$ for all $i, j \in \mathcal{N}_i$ and k).
- 3) The DLKCF with consensus gain as given in (12) (where $\gamma_{i,k}^j = 0.99 \min\{\gamma_{i,k}^*, \gamma_{j,k}^*, \hat{\gamma}_{i,k}^j\}$ with $\hat{c} = 0.01$).

Fig. 1 shows the network setup and the communication topology for the three filters. At time k , the average disagreement \tilde{u}_k of the posterior estimate is computed by $\tilde{u}_k = \frac{1}{N-1} \sum_{i=1}^{N-1} \frac{\|\tilde{u}_{i,k}^{i+1}\|_2^2}{n_{i,i+1}}$ with $\tilde{u}_{i,k}^{i+1} = \hat{I}_{j,i} \boldsymbol{\eta}_{j,k|k} - \hat{I}_{i,j} \boldsymbol{\eta}_{i,k|k}$, and the average estimation error is given by $\boldsymbol{\eta}_k = \frac{1}{N} \sum_{i=1}^N \frac{\|\boldsymbol{\eta}_{i,k|k}\|_2^2}{n_i}$.

Table I reports the disagreement and estimation error of the three filters, where $\tilde{u} = \sum_{k=1}^{k_{\max}} \tilde{u}_k$ and $\boldsymbol{\eta} = \sum_{k=1}^{k_{\max}} \boldsymbol{\eta}_k$ with k_{\max} denoting the total number of time steps. Since the neighboring sections in the LKF have no overlapping cells except the shared boundary cells with sensor measurements, the neighbor dis-

TABLE I
DISAGREEMENT AND ERROR OF ESTIMATE¹

Causes		Disagreement $\tilde{u} (\times 10^{-2})$			Error $\eta (\times 10^{-2})$		
HS	IA	LKF	DLKCF-0	DLKCF	LKF	DLKCF-0	DLKCF
False	–	–	0.294	0.119	0.423	0.349	0.308
True	False	–	0.336	0.119	0.562	0.503	0.468
True	True	–	7.361	4.664	2.941	2.670	2.633

TABLE II
RUNTIME COMPARISON OF THE CENTRAL KF AND DLKCF (PER AGENT)

Central KF			DLKCF			
n	Runtime t_c (s)	n	n_l	\hat{n}	N	Runtime t_d (s)
100	104	100	28	10	5	6.2
210	512	210	50	10	5	24.6
210	512	210	58	20	5	42.2

agreement for the LKF is not considered. It is shown that the estimation accuracy of the LKF is vulnerable to inconsistent error models, since the IA can never identify the high-error sensors they are connected to, while in the DLKCF-0 and DLKCF some of the IA apply the correct measurement error covariance matrices when they share sensor data and sensor models with neighbors. Moreover, compared to the DLKCF-0, adding the consensus term in the DLKCF considerably reduces the neighbor disagreement (regardless of the existence of HS or IA).

As stated in Remark 1, we remove the existence of IA and perform an NEES check [24] of the DLKCF across 50 Monte Carlo runs, thus accessing the validity of dropping the cross correlations among different agents in the estimation error covariance. The average percentage of time steps across all the sections that the NEES measure surpasses the two-sided 95% probability concentration region [1.484, 2.6] is 1.98%. Among all the sections, the maximum (resp. minimum) percentage of time steps that the NEES is greater than the upper limit (resp. smaller than the lower limit) is 2.45% (resp. 1.8%). This indicates that the filter-calculated error covariance matches the mean square error of the DLKCF.

B. Computational Complexity

For simplicity, let $n_i = n_l$ for all i , and denote as \hat{n} the uniform size of the overlapping regions. The computational complexity of the DLKCF for the i th local agent is dominated by $O(n_l^3 + (|\mathcal{N}_i| \hat{n})^3)$ at each time step, where $|\mathcal{N}_i|$ is the number of neighbors of agent i . This implies that we need $\hat{n} < n_l |\mathcal{N}_i|^{-1}$ to have a consensus term with computational complexity less than the LKF. Table II reports the runtime per agent of the DLKCF and the central KF to complete 2000 estimation steps tracking a shockwave on a stretch of freeway, which we denote as t_d and t_c , respectively. It is evident that compared to the central KF, the runtime of the DLKCF is considerably reduced. Moreover, given a fixed network dimension and a fixed number of agents, the computation load increases with the size of the overlapping regions.

VI. CONCLUSION AND FUTURE WORK

In this paper a DLKCF is designed for large-scale multiagent traffic estimation. The DLKCF is applied to the SMM to monitor traffic on a road network partitioned into local sections, with overlapping regions between neighbors introduced to allow for information exchange. We prove that the mean error dynamics of the DLKCF is GAS when all sections switch among observable modes. For an unobservable section, the mean estimates are shown to be ultimately bounded inside the physically meaningful interval. We also prove that the 2-norm of the mean error for any given section is upper bounded under switches among observable and unobservable modes, provided that the section remains observable for a minimum residence time after switching to an observable mode from an unobservable one. Numerical experiments illustrate the effect of the DLKCF on reducing the estimation error, compared to the LKF, as well as promoting agreement among agents. The numerical results also show a considerable reduction on the runtime of the DLKCF compared to a central KF.

To apply the DLKCF in the field, extension of the observability results to freeway networks with junctions is necessary but straightforward. Moreover, the development and incorporation of robustness results on the detection of sensing/computing outliers and model mismatches in each local agent can further improve estimation accuracy.

ACKNOWLEDGMENT

The authors would like to thank Prof. C. Canudas de Wit and the reviewers for constructive suggestions that improved this manuscript.

REFERENCES

- [1] B. S. Y. Rao, H. F. Durrant-Whyte, and J. A. Scheen, "A fully decentralized multi-sensor system for tracking and surveillance," *Int. J. Robot. Res.*, vol. 12, no. 1, pp. 20–44, 1993.
- [2] S. Grime and H. F. Durrant-Whyte, "Data fusion in decentralized sensor networks," *Control Eng. Practice*, vol. 2, no. 5, pp. 849–863, 1994.
- [3] R. Olfati-Saber, "Distributed Kalman filtering for sensor networks," in *Proc. 46th IEEE Conf. Decis. Control*, 2007, pp. 5492–5498.
- [4] R. Olfati-Saber, "Kalman-consensus filter: Optimality, stability, and performance," in *Proc. 48th IEEE Conf. Decis. Control*, 2009, pp. 7036–7042.
- [5] M. A. Demetriou, "Adaptive consensus filters of spatially distributed systems with limited connectivity," in *Proc. 52nd IEEE Conf. Decis. Control*, 2013, pp. 442–447.
- [6] H. Bai, R. A. Freeman, and K. M. Lynch, "Distributed Kalman filtering using the internal model average consensus estimator," in *Proc. Amer. Control Conf.*, 2011, pp. 1500–1505.
- [7] A. Kamal, J. Farrell, and A. Roy-Chowdhury, "Information weighted consensus filters and their application in distributed camera networks," *IEEE Trans. Autom. Control*, vol. 58, no. 12, pp. 3112–3125, Dec. 2013.
- [8] G. Battistelli, L. Chisci, G. Mugnai, A. Farina, and A. Graziano, "Consensus-based linear and nonlinear filtering," *IEEE Trans. Autom. Control*, vol. 60, no. 5, pp. 1410–1415, May 2015.
- [9] U. A. Khan and J. M. F. Moura, "Distributing the Kalman filter for large-scale systems," *IEEE Trans. Signal Process.*, vol. 56, no. 10, pp. 4919–4935, Oct. 2008.
- [10] S. S. Stanković, M. S. Stanković, and D. M. Stipanović, "Consensus based overlapping decentralized estimator," *IEEE Trans. Autom. Control*, vol. 54, no. 2, pp. 410–415, Feb. 2009.
- [11] M. Farina, G. Ferrari-Trecate, and R. Scattolini, "Moving-horizon partition-based state estimation of large-scale systems," *Automatica*, vol. 46, no. 5, pp. 910–918, 2010.

- [12] J. Cortés, “Distributed Kriged Kalman filter for spatial estimation,” *IEEE Trans. Autom. Control*, vol. 54, no. 12, pp. 2816–2827, Dec. 2009.
- [13] S. Blandin, A. Couque, A. Bayen, and D. B. Work, “On sequential data assimilation for scalar macroscopic traffic flow models,” *Phys. D, Nonlinear Phenom.*, vol. 241, no. 17, pp. 1421–1440, 2012.
- [14] L. Munoz, X. Sun, R. Horowitz, and L. Alvarez, “Piecewise-linearized cell transmission model and parameter calibration methodology,” *Transp. Res. Rec.*, vol. 1965, pp. 183–191, 2006.
- [15] I. Morarescu and C. Canudas de Wit, “Highway traffic model-based density estimation,” in *Proc. Amer. Control Conf.*, 2011, vol. 3, pp. 2012–2017.
- [16] C. Canudas de Wit, L. R. Leon Ojeda, and A. Kibangou, “Graph constrained-CTM observer design for the Grenoble south ring,” in *Proc. 13th IFAC Symp. Control Transp. Syst.*, 2012, pp. 197–202.
- [17] A. Zeroual, N. Messai, S. Kechida, and F. Hamdi, “Calibration and validation of a switched linear macroscopic traffic model,” in *Proc. 3rd Int. Conf. Control, Eng. Inf. Technol.*, 2015, pp. 1–5.
- [18] H. T. Banks and K. Kunisch, *Estimation Techniques for Distributed Parameter Systems*. Berlin, Germany: Springer, 2012.
- [19] Y. Sun and D. B. Work, “A distributed local Kalman consensus filter for traffic estimation,” in *Proc. 53rd IEEE Conf. Decis. Control*, 2014, pp. 6484–6491.
- [20] P. I. Richards, “Shock waves on the highway,” *Oper. Res.*, vol. 4, no. 1, pp. 42–51, 1956.
- [21] M. Lighthill and G. Whitham, “On kinematic waves. II. A theory of traffic flow on long crowded roads,” *Proc. Roy. Soc. London Series A, Math. Phys. Sci.*, vol. 229, no. 1178, pp. 317–345, 1955.
- [22] C. F. Daganzo, “The cell transmission model, part II: Network traffic,” *Transp. Res. Part B, Methodol.*, vol. 29, no. 2, pp. 79–93, 1995.
- [23] Y. Sun and D. B. Work, “Scaling the Kalman filter for large-scale traffic estimation,” 2016. arXiv:1608.00917. [Online]. Available: <http://arxiv.org/abs/1608.00917>
- [24] Y. Bar-Shalom, X. R. Li, and T. Kirubarajan, *Estimation with Applications to Tracking and Navigation*, 1st ed. Hoboken, NJ, USA: Wiley, 2001.
- [25] C. Godsil and G. Royle, *Algebraic Graph Theory*. Berlin, Germany: Springer, 2001.
- [26] A. H. Jazwinski, *Stochastic Process and Filtering Theory*. Cambridge, MA, USA: Academic, 1970.
- [27] D. Liberzon, *Switching in Systems and Control*. Berlin, Germany: Springer, 2012.
- [28] D. Xie, H. Zhang, H. Zhang, and B. Wang, “Exponential stability of switched systems with unstable subsystems: A mode-dependent average dwell time approach,” *Circuits Syst. Signal Process.*, vol. 32, no. 6, pp. 3093–3105, 2013.



Ye Sun (M'16) received the B.E. degree from Tsinghua University, Beijing, China, in 2012 and the M.S. degree from the University of Illinois at Urbana-Champaign, Urbana, IL, USA, in 2014, both in civil engineering. She is currently working toward the Ph.D. degree in civil engineering at Civil and Environmental Engineering and Coordinated Science Laboratory, the University of Illinois at Urbana-Champaign.

Her research interests include distributed estimation of large-scale transportation systems, adaptive sensing, and decentralized control of cyber physical systems.



Daniel B. Work (M'16) received the B.S. degree in civil engineering from the Ohio State University, Columbus, OH, USA, in 2006. He received the M.S. and Ph.D. degrees from the University of California, Berkeley, CA, USA, both in civil engineering, in 2007 and 2010, respectively.

He is currently an Assistant Professor at Civil and Environmental Engineering and Coordinated Science Laboratory, University of Illinois at Urbana-Champaign, Urbana, IL, USA. His research interests include control and estimation problems in civil

engineering.

Prof. Work received the NSF CAREER Award in 2014 and the IEEE ITSS Best Dissertation Award in 2011.